12-2009

Wide Area Monitoring and Control

Manish Patel
Clemson University, mpatel@clemson.edu

WIDE AREA MONITORING AND CONTROL

A Dissertation
Presented to
the Graduate School of
Clemson University

In Partial Fulfillment
of the Requirements for the Degree
Doctor of Philosophy
Electrical Engineering

---

by
Manish Patel
December 2009

Accepted by:
Dr. Adly A. Girgis, Committee Chair
Dr. Elham B. Makram
Dr. Ian D. Walker
Dr. Hyesuk K. Lee

ABSTRACT

Today's interconnected power system is deregulated for wholesale power transfers. In 1996 Federal Energy Regulatory Commission provided open access of the transmission network to utilities. Since then utilities are transferring power over long distances to bring reliable and economical electric supply to their customers. As the number of wholesale power transactions taking place over an interconnected system are increasing, system operators in control areas are forced to monitor the grid on a large scale to operate it reliably. Before scheduling such a large scale power transactions, it is necessary to make sure that such transaction will not violate system operating steady state security limits such as transmission line-flow limits and bus voltage limits. The ideal solution to this problem is to consider entire interconnected system as one system to monitor it. However, this solution is technically expensive if not impossible and hindered by confidentiality issues.

This research aims to develop tools that help the system operators to operate the deregulated power grid reliably. State estimation is the tool used by today's energy control centers to develop a base case of the system in real-time, which is further used to study the impact of disturbances and power transactions on static and dynamic security limits of the system. In order to monitor the deregulated power system, a wide area state estimator is required. In this dissertation a two-level approach to achieve such a solution is presented. This way, individual areas are allowed to run their own state estimator, without exchanging any real-time data with neighbor areas. The central coordinator then coordinates state estimator results available from individual areas to bring them to a

global reference. This dissertation also presents the application of measurements from GPS synchronized phasor measurement units to improve accuracy of two-level state estimator.

In addition to monitoring, system operators also need to determine that if they can allow the scheduled transaction to take place. This requires them to determine transfer capability of the system in real-time. This dissertation presents new iterative transfer capability algorithm which can be used in real-time. As an interconnected system is deregulated and the power transactions are taking place through many control areas, a system wide solution of transfer capability is required. This dissertation presents a two-level framework similar to one used for state estimation to achieve multi-area transfer capability solution. In general, the research work carried out would help in improving power system reliability and operation.

DEDICATION

This dissertation is dedicated to *My Parents*, for their support and encouragement, *Ketal*, my wife for her patience, *Ayushi and Shreya*, my daughters and *friends* without whom this would not have been possible.

ACKNOWLEDGMENTS

I would like to express my sincere gratitude and appreciation to my advisor Dr. Adly A. Girgis for his guidance throughout this research. I am grateful for his support and especially patience during the entire period of this research. I would also like to thank Dr. Elham B. Makram, Dr. Ian D. Walker and Dr. Hyesuk K. Lee for serving on my advisory committee.

I would like to thank Clemson University Electrical Power Research Association (CUEPRA) and the Electrical and Computer Engineering (ECE) Department at Clemson University for their financial support.

I would like to thank all my colleagues in the power group for their professional and friendly relationship.

Finally, I would like to thank my parents and wife for their support, patience and encouragement when it was most required.

.

TABLE OF CONTENTS

Page

Table of Contents (Continued)

Page

LIST OF TABLES

List of Tables (Continued)

Table Page

LIST OF FIGURES

CHAPTER ONE

INTRODUCTION

1.1 Motivation

The electric power industry is undergoing multiple changes and restructuring towards deregulation. As the restructuring is happening profits are less guaranteed and some electric power utilities are increasing the loads on the grid to generate more revenue. This creates the need for system operators to know the exact operating state of the system in real-time.

In 1996, Federal Energy Regulatory Commission (FERC) issued Order No. 888 [1], which opened wholesale electric power sales to competition. FERC provided a non discriminatory open access of the transmission system to all utilities. Since then increase in wholesale power transactions is observed and are expected to grow in future as well. Today's interconnected power system is divided into many control areas; each controlled by their own control center and is deregulated.

The northeast blackout of 2003 was in part caused by the national electric grid being pushed past its limits and the operators not detecting that the grid was in a critical state [2, 3]. If the operators of the electric grid in Ohio had been able to detect that several areas of their grid were in critical states, they might have been able to prevent the cascading events which followed in neighboring states of Michigan, Pennsylvania, New York, Vermont, Massachusetts, Connecticut, New Jersey and the Canadian state of Ontario. The total estimated losses were between 4 to 10 billion dollars.

As the number of wholesale power transactions taking place over an interconnected system, which may involve more than just buyer and seller areas, are increasing, system operators in control areas are forced to monitor the grid on a large scale to operate it reliably. Before scheduling such a large scale power transactions, it is necessary to make sure that such transaction will not violate system operating steady state security limits such as transmission line-flow limits and bus voltage limits. Also it is necessary to make sure that large disturbances such as faults, loss or acquisition of generation, loss or acquisition of loads etc will not result into power system instability. So it is very important that not only the buyer and seller of the transaction but each area involved with the transaction ensures that the execution of the transaction occurs within the limits of not only static security limits but also the dynamic security limits.

The cascading event in power systems is usually divided into three steps: initiating event, slow progression and fast progression. The initiating event is usually a random event and is a failure of one or more component (transmission line, generator, and transformer) of the power system happening at different times. The failure of system components during the initiating event may cause rest of the system components to overload to meet the load demand. As a result of overload, those components eventually will trip out and push the rest of the components beyond their capacity. This is called a slow progression of a cascading event. Until up to a point when transmission system cannot supply the demand and run into either voltage instability or angular instability, which is referred as fast progression and thereby will take down the entire system in very short time. Figure 1.1 presents the initiating event, slow progression and fast progression

of the August 14, 2003 blackout [3]. Initiating events and slow progression are the time periods in which operators in control center can take corrective actions to avoid or at least reduce the impact of cascading failure on the system.

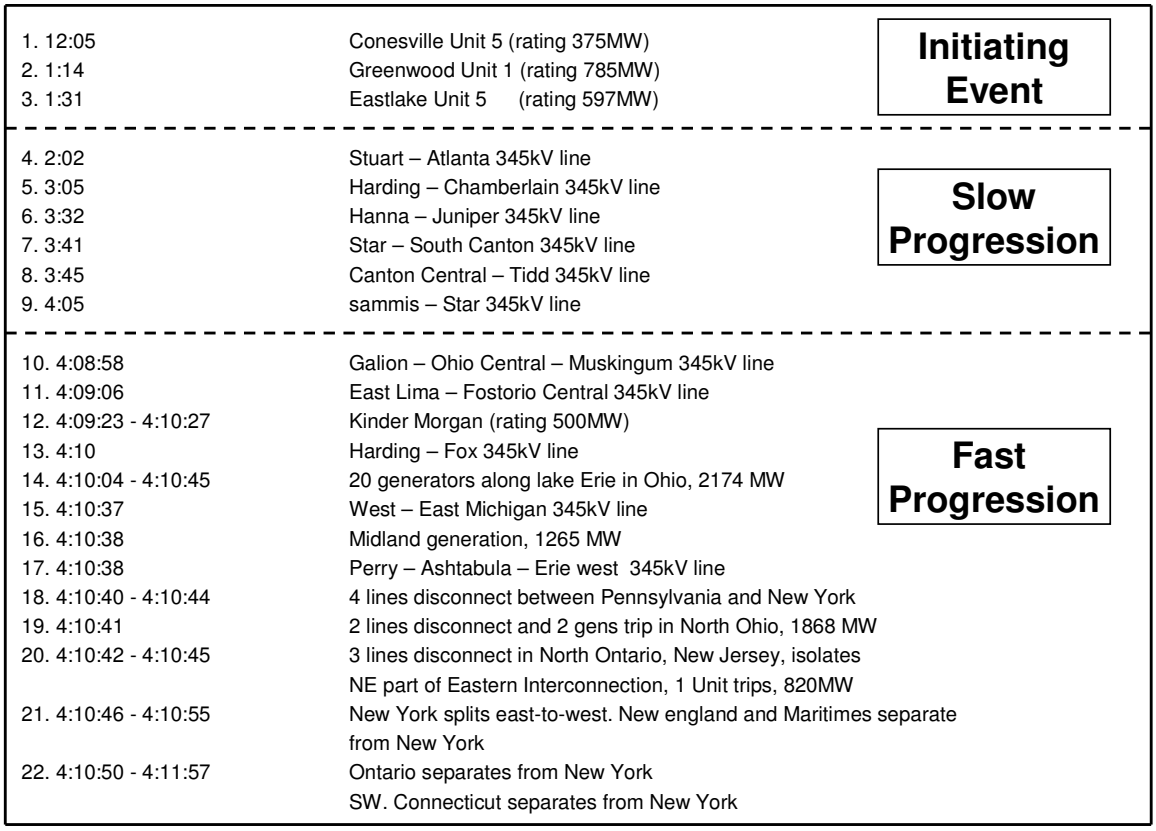

Figure 1.1: Initiating events, slow and fast progression of August 14, 2003 blackout

This research aims to develop tools that help the system operators to operate the deregulated power grid reliably. Indirectly, it should also help operators to identify the happening of cascading failure during the very early stages. State estimation is the tool used by today's modern energy control centers to develop a base case of the system in real-time, which is further used to study the impact of disturbances and power

transactions on static and dynamic security limits of the system. State estimation is considered a backbone of real-time security analysis. Figure 1.2 refers to the applications of state estimator in control center.

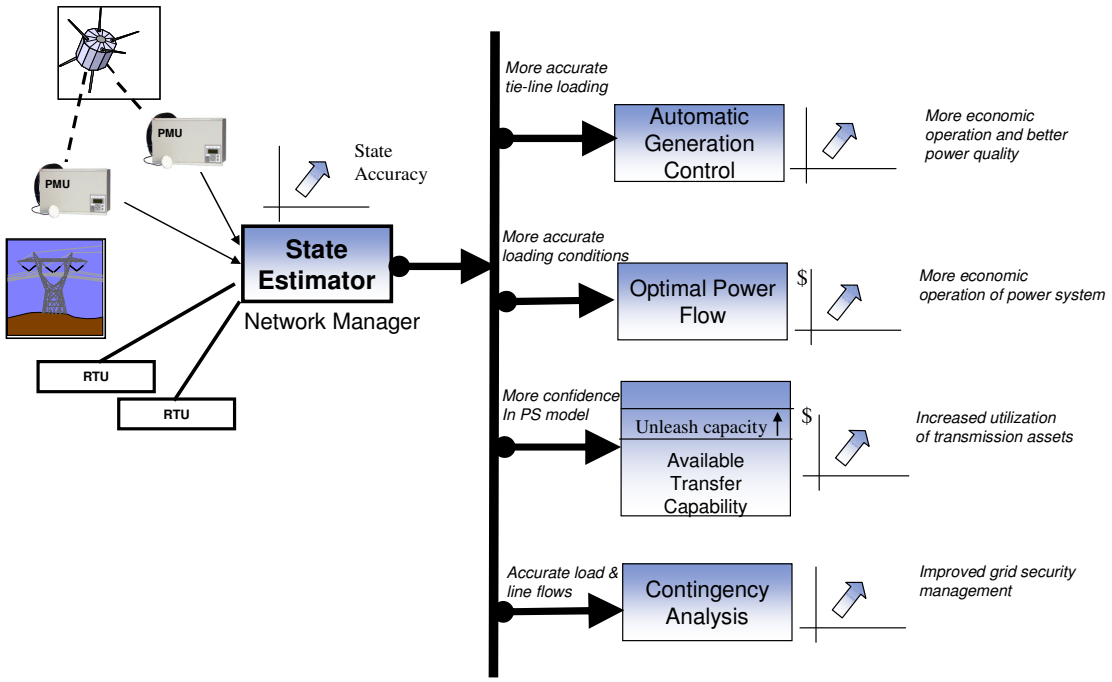

Figure1.2: Applications of state estimator in control center

The raw information available as measurements from the system through Supervisory Control and Data Acquisition (SCADA) are processed by the state estimator, which provides the best estimate of the operating state of the system. In order to monitor the large scale power transactions taking place over an interconnected system, a Wide Area State Estimator (WASE) is required. There are mainly two approaches to implement wide area state estimation.

1. By modeling the neighbor utilities in detail and accurately in one's own state estimation – External Network Modeling (ENM).
2. To get the output of state estimators from each area and to coordinate them to a global reference – Variant of Hierarchical State Estimation (HSE) or Two-Level State Estimation (TLSE).

External network modeling requires a great deal of effort in maintaining a huge measurement set and topology information. The basic idea is to collect real-time measurements and topology information from each area and run state estimator for the entire interconnected area on one computer [4-7]. The topology of the system is dynamic as there are transformer and line changes due to both forced and maintenance outages on a minute to minute basis. Also the system model changes because of addition or retirement of equipments in the system. Because of the effort in maintaining and ensuring the data quality to the state estimator, there is a tendency to minimize the data used from neighboring systems in the state estimator. Also, most of the utilities are reluctant to share their real-time data with neighbor utilities because of confidentiality issues. Loss of significant data from any part of observed interconnected system can result in the failure of state estimator for the entire interconnected system. This problem was experienced during August 14, 2003 blackout [2, 3]. At 14:02 EDT, Dayton Power & Light's (DPL) Stuart-Atlanta 345-kV line tripped due to a tree contact, which did affect Midwest Independent System Operator's (MISO's) performance as reliability coordinator. MISO's state estimator was unable to assess system conditions for most of the period between 12:15 and 15:34 EDT, due to a combination of human error and the effect of the loss of

DPL's Stuart-Atlanta line on other MISO lines as reflected in the state estimator's calculations. Without an effective state estimator, MISO was unable to perform contingency analysis of generation and line losses within its reliability zone. Because of disadvantages mentioned, generally network modeling is not a recommended method for wide area state estimation.

The second approach overcomes these disadvantages as it requires a central coordinator to assemble the state estimator outputs from each area to achieve wide area state estimation, widely known as two-level state estimation [8-10]. This approach has been investigated in the past for the purpose of reducing computational time, memory requirements and amount of data exchange. There are several issues, which need to be addressed for this approach to work. Some of the issues can be resolved by establishing procedures for each area to follow while others require new analysis methods. The first issue is that of overlap. Each area uses a state estimator model which includes their external network. Mostly, the external network is the reduced model of their neighbor utilities, which should be removed for this approach. The second issue is time synchronization of the data. The overall solution of the wide area state estimator can be improved if all individual areas agree to run their local state estimator at the same clock time. Measurements available from GPS synchronized Phasor Measurement Units (PMUs) can also be used to improve the accuracy of the state estimator [11]. The final question needs to be addressed is that what happens when an individual area state estimator fails to converge. In this case, the wide area state estimator may continue to converge with the area missing. If for any reason, wide area state estimator doesn't

converge without the missing area, then it may be possible to use the model of the missing area from the last converged case, which would allow the wide area state estimator to converge. However, this may produce inaccurate estimate of the states near the boundaries of the missing area.

As mentioned earlier, in 1996 since FERC provided open access of the transmission network [1], large scale power transactions between utilities have increased and will increase more in future, in order to provide reliable and economical electric supply. For example, hydroelectric power generated in Canada can be transferred to consumers and industry in Los Angeles using the high voltage transmission system. In large networks, this may involve more than one control area. In such situations, system operators need answer to a question, "How much power can be transmitted reliably between two buses of an interconnected system?" Available Transfer Capability (ATC) and Total Transfer Capability (TTC) can provide system operators useful information regarding the total power transfer possible between two nodes without hindering the reliability of the system.

The Federal Energy Regulatory Commission requires that the available transfer capability information should be made available on a publicly accessible Open Access Information Sharing System (OAISS) on a real-time basis [12]. ATC is defined as a measure of the transfer capability, in the physical transmission network, for transfer of power over and above already committed uses. According to North American Electric Reliability Corporation's (NERC) definition, total transfer capability indicates the amount of power that can be transferred between two buses (or groups of buses) in the

system in a reliable manner in a given time frame [12, 13]. The total transfer capability is the largest flow for which there are no thermal overloads, voltage limit violations, voltage collapse and/or any other system security problems such as transient stability. The TTC minus the base case flow and appropriate transmission margin is the ATC. The base case used to calculate ATC may be obtained from real-time state estimator or the contingency case. The ATC problem is the determination of the largest additional amount of power above some base case value that can be transferred in a prescribed manner between two sets of buses: the source, in which power injections are increased, and the sink, in which power injections are decreased by same amount.

The existing methods for ATC calculations are based on DC/AC-Power Transfer Distribution Factors (PTDFs) [14-15], Continuation Power Flow (CPF) [16-17] or Optimal Power Flow (OPF) [18-19]. The detailed review of these methods is presented in chapter 3.

To summarize, DC-PTDFs are based on system topology only and hence do not produce accurate ATC results. AC-PTDFs are based on current operating state of the system, but they do not consider either generator limits or bus voltage limits while calculating ATC. CPF based methods require repeated solution of power flow and hence they are very slow and cannot be used in real-time. OPF based methods are also slow as an optimization problem becomes very time consuming for large systems. Because of the limitations of the existing methods, none of them are suitable for ATC calculation in real-time basis. Hence, there is a need to develop new algorithm for ATC calculation which is fast and accurate and can be used in real-time.

In today's deregulated interconnected system, operators are required to calculate ATC of an interconnected system instead of just for their own area. To keep the data exchange minimum, there is a need to develop an ATC calculation algorithm based on hierarchical structure. This concept is new for ATC calculation but is similar to two-level state estimator. At the first level, individual areas calculate their own ATC value for the given system conditions and transfer the results to central coordinator. Central coordinator then coordinates the results obtained from each area and issues ATC value for an interconnected system for a given power transaction.

1.2 Research Objectives/Contributions

This research aims to developing new algorithms for wide area state estimation and available transfer capability calculations for an interconnected power system consisting of many control areas. Two-level hierarchical approach is adopted for both as it has many advantages for today's deregulated power system. The primary motives are as follows.

1. Development of two-level state estimation algorithm to achieve wide area state estimation of an interconnected power grid. This way, individual areas are allowed to run their own state estimator, without exchanging any real-time data with neighbor areas. The central coordinator then coordinates state estimator results available from individual areas to bring them to a global reference. Generally, use of boundary injection measurements at coordinator level requires some real-time exchange between individual areas and coordinator other than just

state estimator results. The use of modified power injections at coordinator level is proposed and implemented to increase the redundancy and hence accuracy of coordinator level.

2. Development of a state estimator to include the measurements available from GPS synchronized PMUs to increase the accuracy of estimation. Existence of short or low impedance transmission lines in a boundary network introduces errors in estimation results of two-level state estimator. PMU measurements are used at those boundary buses to reduce the estimation errors.

3. Development of an accurate and fast method to calculate available transfer capability of the power system. Existing ATC calculation methods either uses AC/DC-PTDFs or OPF and CPF, which are not accurate and slow respectively. The proposed iterative method is accurate compared to methods based on AC/DC-PTDFs and faster compare to OPF or CPF based methods.

4. Development of two-level transfer capability algorithm to achieve ATC of an interconnected power system. As explained for wide area state estimator, individual areas calculates ATC of their own system for a given power transaction. Central coordinator then coordinates results of each area to obtain multi-area ATC value. The developed method uses REI-equivalents to keep the data exchange minimum between control areas.

CHAPTER TWO

MULTI-AREA STATE ESTIMATION

This chapter presents mathematical background of state estimation and proposes a new algorithm based on two-level state estimator to achieve wide area state estimation. The use of measurements from Phasor Measurement Units (PMUs) is becoming very common to the power system for various applications. They can also be used for state estimation. This chapter presents and discusses methods to include PMU measurements in state estimator. The use of PMU measurements to improve the accuracy of Wide Area State Estimator (WASE) is also presented. Finally, this chapter also shows the effect of system decomposition on Two-Level State Estimation (TLSE).

2.1 Power System State Estimation

State estimation in power system is used to build realistic and reliable real-time model of the power network. It is the backbone of online security analysis in energy control centers. It acts like a filter between the raw information received from the system and all application functions that need the reliable data of the current state of the system.

In power systems, the measurements are collected using Supervisory Control and Data Acquisition (SCADA) system. These measurements are not always complete and accurate. Sometimes, there is also a possibility of bad measurement and hence the real-time AC power flow cannot be extracted from these measurements. The state estimation uses the available measurements from SCADA as well as the circuit breaker status, tap

positions of transformers, parameters of transmission lines, transformers, shunt reactors and capacitors to estimate the best state of the system [20, 21]. The state variables in this process are the voltage magnitudes and relative phase angles at each bus of the power system. The commonly used measurements for state estimation are as follows:

1. Power flows: real and reactive power flow through the transmission line.
2. Power injections: real and reactive power injected at the buses.
3. Voltage magnitude: voltage magnitude measurements at the system buses.
4. Current magnitude: current magnitude flowing through the transmission lines.
5. Synchronized Phasor Measurements: they can be in form of voltage phasors and current phasors.

The measurements in the system are assumed to have the errors which have a Gaussian distribution with zero mean. These measurements can be expressed as

$$z_m = h_m(x) + e_m \qquad (2.1)$$

where,

z_m measured value of the i^{th} measurement.

$h_m(x)$ non-linear function relating error free measurement to the state vector

e_m random measurement error

The state vector generally includes voltage magnitudes and angles of all system buses except the reference bus angle. Hence for the 'n' bus system, the total number of state variables is (2n-1).

$$x^T = [x_1, x_2, ..., x_{2n-1}] \qquad (2.2)$$

Because the measurement errors are independent and assumed to have a normal distribution with zero mean,

$$E(e) = 0$$
$$E(e\ e^T) = R = diag\{\sigma_1^2, \sigma_2^2, ..., \sigma_m^2\}$$

where, σ_i is the standard deviation of ith measurement.

The Weighted Least Square (WLS) state estimator will minimize the following objective function.

$$J(x) = \sum_{i=1}^{m} (z_i - h_i(x))^2 / R_{ii} = [z - h(x)]^T R^{-1} [z - h(x)] \quad (2.3)$$

In order to solve the above equation, the first order optimality conditions will have to be satisfied. These can be expressed as

$$g(x) = \frac{\partial J(x)}{\partial x} = -2H^T(x)R^{-1}[z - h(x)] \quad (2.4)$$

where,

$$H(x) = \frac{\partial h(x)}{\partial x}$$

Using Newton's method to make *g(x)* equal to zero.

$$\Delta x = [\frac{\partial g(x)}{\partial x}]^{-1}[-g(x)] \quad (2.5)$$

The Jacobin of *g(x)* is calculated by treating *H(x)* as a constant matrix, which is true for a given state vector *x*. Substituting 2.4 into 2.5.

$$\Delta x = [H^T(x)R^{-1}H(x)]^{-1}H^T(x)R^{-1}[z - h(x)] \qquad (2.6)$$

The above non-linear equation can be solved using iterative Newton method until Δx is very small and tends to zero. .

$$x^{k+1} = x^k + [G(x^k)]^{-1} * g(x^k) \qquad (2.7)$$

where,

k is the iteration index

$\boldsymbol{x^k}$ is solution vector at iteration k and

$$G(x^k) = \frac{\partial g(x^k)}{\partial x} = H^T(x^k)R^{-1}H(x^k)$$
$$g(x^k) = H^T(x^k)R^{-1}[z - h(x^k)]$$

G(x) is called the gain matrix. If the system is fully observable, the gain matrix will be positive definite and symmetric.

2.2 Accuracy Test Matrices

Following test metrics are used to determine the performance of state estimation results. These metrics are developed by KEMA and are recommended to determine the performance of state estimator [22].

$$Macc_V = \left\| \vec{V}_{error} \right\|_2 = \left(\sum_{j=1}^{nbus} \left| \vec{V}_j^{true} - \vec{V}_j^{est} \right|^2 \right)^{1/2} \quad (2.8)$$

$$\left\| P_{error} \right\|_1 = \sum_{j=1}^{nbranch} \left| P_j^{true} - P_j^{est} \right| \quad (2.9)$$

$$\left\| P_{error} \right\|_\infty = \max_{\text{j=1....nbranch}} \left| P_j^{true} - P_j^{est} \right| \quad (2.10)$$

where,

nbus total number of buses in the system

nbranch total number of branches in the system

$\boldsymbol{P_j}$ active power flow in j^{th} branch

$\vec{\boldsymbol{V}}_j$ complex phasor voltage of j^{th} bus

Equation (2.8) represents the second norm of the complex phasor voltage estimation error. It is important that the same reference bus be used for both 'true' and 'estimated' voltages. Equation (2.9) is the 1-norm of the estimation error for active power flows and is proportional to the average error in branch flow estimation. Equation (2.10) is the infinity norm of the estimation error and represents the worst case error. It is important to know that metrics shown in equation (2.9) and (2.10) are sensitive to model of the system, but they are useful to compare different algorithms for a fixed network model. All three metrics seem reasonable and larger values indicate worse performance.

2.3 Application of PMU Measurements in State Estimation

GPS synchronized phasor measurement units are not new to the power system. The advancements in recent communication technology have made the use of PMU measurements in power system very common. The measurements obtained using PMUs are considered to be highly accurate with the accuracy level of 0.01% for magnitude measurements and 0.02 degrees for angle measurements. Also, these measurements are taken at the same time stamp so they do not have errors introduced due to time skewness. Generally, PMUs are synchronized to within 0.2 micro-second and are available with the reliability of 99.87% [23].

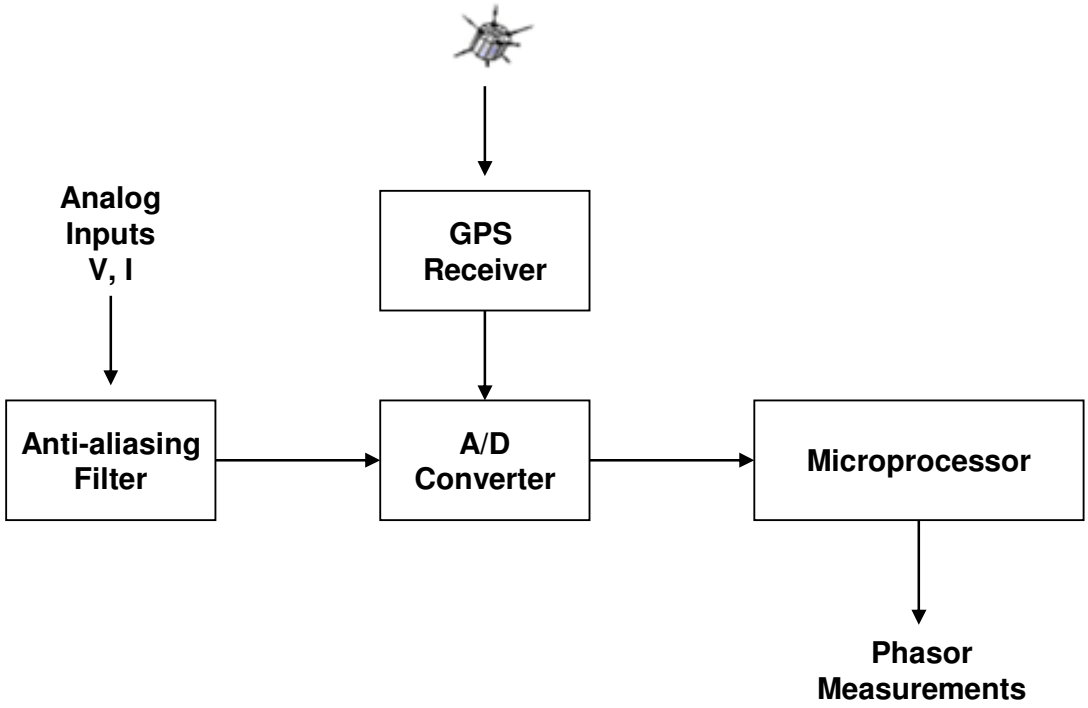

Figure 2.1: Block Diagram of PMU

Figure 2.1 shows the functional block diagram of the PMU. The GPS receiver provides the synchronization signal to A/D transformer, and the voltage or current analog signals are input into A/D transformer through an anti-aliasing and surge filter. The microprocessor determines the phasor of the voltage or current with respect to the reference according to the digital signal from the A/D transformer.

Recent papers have indicated that the state estimator performance can be improved significantly, if PMU measurements are used in state estimator [11, 24-25]. The traditional approach to use PMU measurements in state estimation is to input the SCADA measurements and PMU measurements together in state estimator. However, there are two disadvantages of this approach. One is that if the number of PMU measurements is very small compare to traditional SCADA measurements then state estimator results would not really reflect the advantage of using PMU measurements. Second issue is that current existing state estimation programs in energy control centers are not designed to handle the PMU measurements. These programs either needs upgrading or needs to be replaced by the newer ones to incorporate PMU measurements into state estimator.

The second approach avoids the necessity of changing the existing state estimation program in energy control centers. The approach is such that it will allow traditional state estimator to function just as before. The output of the traditional state estimator is processed by another linear estimator to incorporate PMU data and is then put back in the same format as that produced by the traditional state estimator to be used by rest of the control center applications. In this approach, PMU measurements are

excluded from a traditional state estimator, but they are integrated with traditional state estimator results by means of linear state estimation. Because the second step is linear state estimator, it is fast and does not add any significant time delay. Figure 2.2 describes the hybrid state estimator.

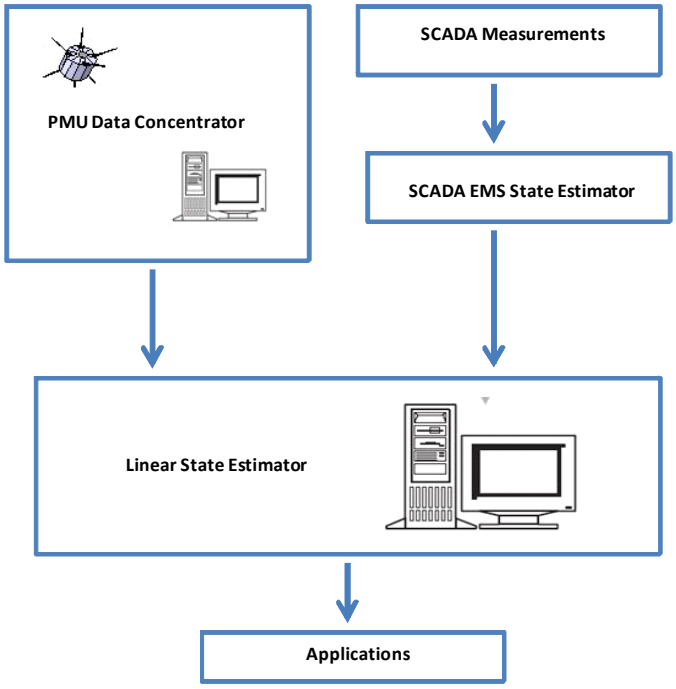

Figure 2.2: Hybrid State Estimator

2.3.1 Simulation Results – IEEE 118-Bus System

IEEE 118-bus system is used as the test system. The traditional measurements used are voltage magnitudes, power flows and power injections from throughout the system and it is assumed that these measurements have a standard deviation of 1.0%, 1.5% and 3.0% respectively. Besides, 20 buses of the system are assumed to have PMUs

installed, which can provide voltage and current phasors as measurements with the standard deviation of 0.01%. Table 2.1 presents the simulation results for traditional state estimator with and without PMU measurements and hybrid state estimator.

Table 2.1 Comparison of State Estimator Performance
in presence of PMU Measurements

	Traditional SE without PMU Measurements	Traditional SE with PMU Measurements	Hybrid SE with PMU Measurements
$Macc_v$	0.0017 PU	0.0011 PU	0.0010 PU
$\|\|P_{error}\|\|_1$	2.8117 MW	2.7271 MW	2.7521 MW
$\|\|P_{error}\|\|_\infty$	0.0709 MW	0.0623 MW	0.0611 MW

The simulation results show that the use of PMU measurements in state estimator improves its accuracy, regardless of which approach is used to process the PMU measurements. However, the results of traditional and hybrid state estimators are comparable. The hybrid state estimation results are only slightly better than traditional state estimator results. But the difference in accuracy of results may become significant if fewer PMU measurements are used. The flexibility offered by hybrid state estimator makes it more favorable over traditional state estimator as it does not require making changes to existing state estimators.

2.4 Two-Level State Estimation

In today's interconnected power system, the number of power transactions taking place over large distances, which involves many control areas has increased and are expected to grow in future [1]. In this situation, the operators in control centers are forced to monitor the grid on a large scale to operate it reliably. In energy control centers the raw measurements obtained through the SCADA system from the grid are processed by the state estimator, which provides the estimate of the operating state of the system. In order to monitor the large scale power transactions taking place over many areas, a wide area state estimator is required.

There are mainly two approaches to carry out wide area state estimator. First of these, is to model the neighboring utilities in detail and accurately in one's own state estimator. Second, is to obtain the state estimation outputs from each area and convert them to a global reference, known as the hierarchical state estimation. The first approach requires a great deal of effort in maintaining a huge measurement set and topology information. Also, the loss of data from any observed part of the system will result into a total failure of state estimation, which was the case during the august 14, 2003 blackout [2, 3]. This approach also fails when the utilities are reluctant to share their real-time information with neighboring utilities. The second approach overcomes these disadvantages as it requires a central coordinator to assemble the state estimation output from each utility to achieve wide area state estimator.

This kind of hierarchical approach has been investigated in the past with the objective of reducing computational time, memory requirements and amount of data

exchange. The to-date proposed schemes can be classified broadly as two categories: sub-optimal methods and optimal methods. The sub-optimal methods are those in which the overall system is physically parsed into a number of smaller sub-systems each assigned a control center, where in each the state estimation is solved independently. The central computer is mainly used for co-ordination. These methods fit well with the strategies of hierarchical and decentralized control of power systems [8-11, 25-29]. The data transmission involved with these methods is minimal between local and central computers. Depending upon the decomposition strategy adopted in the algorithm, boundary injections and tie-line measurements are ignored at either level of the algorithm. This may introduce high errors in the estimates of the boundary bus states.

The second category of methods is one which determines the state of the system by applying some form of decomposition to the overall system state estimation problem and is known as optimal methods. It parses the overall state estimation problem into a number of sub-problems. Each of these sub-problems is solved using local computers. The intermediate results are sent to the central computer to complete the state estimation process [30-33]. These methods do involve very large amount of data transmission between the local and central computers which somewhat limits their applicability. In today's deregulated power system, utilities are reluctant to share their real-time data with each other as they are part of competitive wholesale power market, which makes optimal approach for wide area state estimation unacceptable.

Van- Cutsem et al [10, 26] proposed several sub-optimal hierarchical state estimation algorithms. They suggested a two-level state estimation algorithm by dividing

the system into ‘k’ non overlapped areas which are connected through tie-lines. In lower level, each area performs state estimation independently with respect to the local reference. In the upper level, the boundary bus states are re-estimated and all the phase angles are coordinated to a global reference. Kobayashi et al [27] proposed the two-level state estimation algorithm based on model coordination method for a system decomposed into ‘k’ non-overlapped areas connected through tie-lines. Kurzyn [8] proposed an algorithm for ‘k’ non-overlapped systems which at the second level does not re-estimate the boundary bus states. Wallach, Handschin and bongers [9] proposed the one level state estimation. The decomposition of the system is done in such a way that the areas are overlapped.

In the previous work, mentioned above, they have difficulty using the boundary injection measurements in the state estimation. Zhao [11] proposed an algorithm in which the boundary injection measurements can be used by using the overlapped areas. The algorithm also proposed detection of any bad boundary injection measurements in upper level if it is not possible to identify them in the lower level because of low redundancy of boundary measurements. But this requires transferring the topology of transmission lines connected to the boundary buses to the central entity, so that injection measurements can be used in the upper level of the algorithm.

2.4.1 System Decomposition

Consider an interconnected system with N areas shown in Fig. 2.3. Individual areas are connected to each other through the tie-line network and the areas are

considered to be overlapping, i.e., Area 1 will not restrict its model to buses A1-1 and A1-2, but will also include buses A2-2 and AN-2 from Areas 2 and N respectively, which is shown in Fig. 2.3. All the area follow similar scheme. The buses in each area can be categorized as internal buses, internal boundary buses and external boundary buses. For example, in Area 1, A1-1 is internal bus, A1-2 is internal boundary bus and A2-2 and AN-2 are external boundary buses.

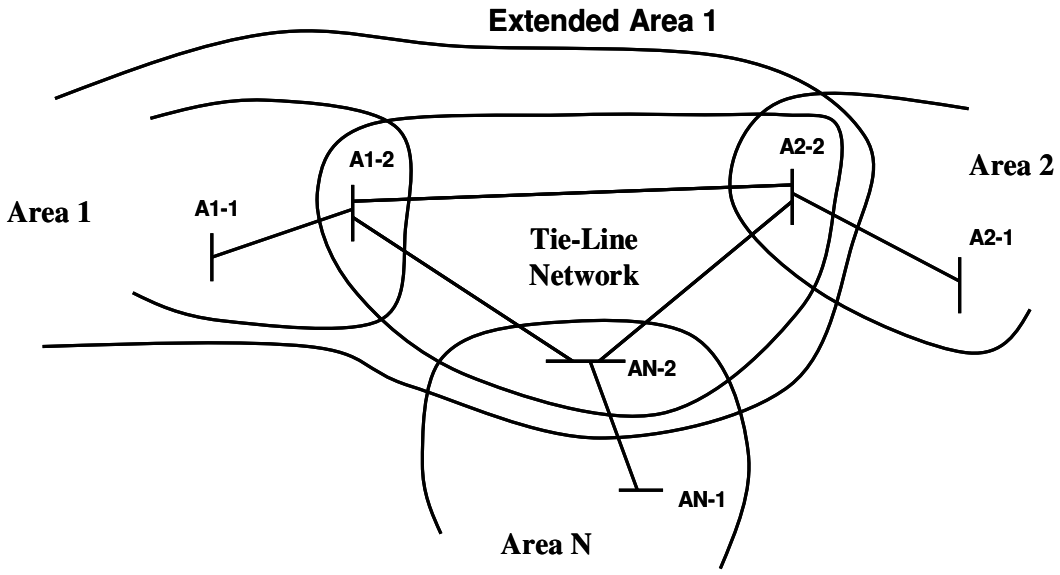

Figure 2.3: System Decomposition - Overlapped Systems

2.4.2 Individual Area State Estimator

It is assumed that each area performs a state estimation using its own measurements. Also, each area can use any special state estimation algorithm as they do not interact with each other. However, individual area state estimators are responsible for detecting and identifying any bad measurements present in their own measurement set.

For simulation it is assumed that each area uses the typical weighted least square estimation algorithm. The commonly used measurements for state estimation are power flows and injections, voltage magnitudes and current magnitudes. Based on system decomposition, the state vector for individual area 'i', at the first level, can be written as

$$x_i^T = [x_i^{\text{int}}, x_{i,b}^{\text{int}}, x_{i,b}^{ext}] \qquad (2.11)$$

where,

x_i^{int} internal bus states of the i^{th} area

$x_{i,b}^{int}$ internal boundary bus states of the i^{th} area

$x_{i,b}^{ext}$ external boundary bus states of the i^{th} area

2.4.3 Wide Area State Estimator

The primary function of the central entity is to collect the state estimation results from each participating area and to find the estimate of an interconnected system with respect to one global reference. In this process, the central entity can use the measurements available from the boundary network such as tie-line power flows, boundary bus injections, boundary bus voltages etc. The central entity also uses the boundary bus states available from individual area state estimators as pseudo measurements to increase the redundancy. Though, the use of boundary bus injection measurements requires each area to transfer the topology and line data information of the lines connected to the boundary buses to the central entity. For example, to use the injection measurement of bus A1-2 in Fig. 2.3, area 1 has to transfer the topology and line data information of the line from A1-1 to A1-2 to the central coordinator. To

overcome this issue, a use of modified power injection measurement is suggested at the second stage. For bus A1-2, the modified active power injection measurement can be written as,

$$P_{A1-2}^{\text{mod}} = P_{A1-2}^{act} - P_{A1-2,A1-1}^{estimated} \tag{2.12}$$

The modified power injection is basically the power injected into the boundary network. In addition to coordinating the state estimation results from each area, the central entity also re-estimates the boundary bus states. This is essential to detect and identify any bad data present in the boundary network, which may have gone undetected at the first level because of low redundancy of measurements near the boundary buses. In this case, the state vector of the central coordinator is defined as

$$x_C = [U^T, x_b^T] \tag{2.13}$$

where,

$U = [u_2, u_3, ..., u_N]^T$

$x_b = [x_{1,b}, x_{2,b}, ..., x_{N,b}]^T$

$\boldsymbol{u_i}$ is the phase angle of i^{th} area reference bus with respect to the global reference. Area 1 reference bus is arbitrarily chosen as the global reference bus. The measurement set available for the central coordinator is given as

$$z_C = [z_b, \hat{x}_b^{\text{int}}, \hat{x}_b^{ext}] \tag{2.14}$$

where,

$$\hat{x}_b^{\text{int}} = [\hat{x}_{1,b}^{\text{int}}, \hat{x}_{2,b}^{\text{int}}, ..., \hat{x}_{N,b}^{\text{int}}]$$
$$\hat{x}_b^{ext} = [\hat{x}_{1,b}^{ext}, \hat{x}_{2,b}^{ext}, ..., \hat{x}_{N,b}^{ext}]$$

z_b is the set of boundary measurements which may include tie-line power flows, modified injection and voltage measurements at the boundary buses. The corresponding measurement model is

$$z_C = h_C(x_C) + e_C \tag{2.15}$$
$$E(e_C) = 0 \qquad E(e_C e_C^T) = R_C \tag{2.16}$$

where,

h_c non-linear function of x_c;

e_c error vector of measurements;

The second level of the algorithm requires minimizing following objective function.

$$J_C = [z_C - h_C(x_C)]^T R_C^{-1} [z_C - h_C(x_C)] \tag{2.17}$$

As the boundary bus states from each area are used as pseudo-measurements at the second level, each individual area is also required to transfer the state covariance matrix along with the boundary bus states to the coordinator. Figure 2.4 represents the block diagram of the algorithm.

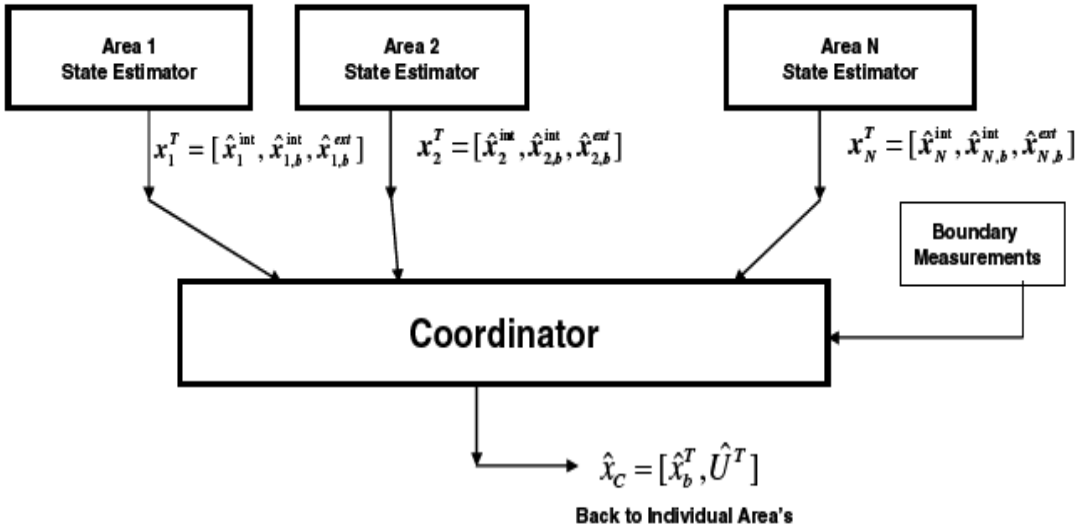

Figure 2.4: Block Diagram of Two-Level State Estimator

2.4.4 Simulation Results IEEE 30-Bus System

IEEE 30-bus system is partitioned into two areas for the simulation purposes. Area 1 consists of buses 1-15 and area 2 consists of buses 16-30. There are 13 boundary buses in total out of which 5 belongs to area 1 and 8 belongs to area 2. In both of the following cases, 7 voltage, 16 pair of power injections and 41 pair of power flow measurements are used. The total number of states at the first level is (2*15-1) = 29 for both areas. At the second level, the total number of states is 1 + 2*13 = 27, which corresponds to 13 boundary bus states and area 2 slack bus. Area 1 slack bus is chosen as a global reference.

Case 1: All the measurements used for state estimation are added with random errors with zero mean and a standard deviation of 0.5% for voltage measurements, 1.0% for

power flow measurements and 1.5% for power injection measurements. Table 2.2 shows the results obtained by integrated and two-level state estimators obtained for the same measurement set.

Table 2.2 SE Results with 0.5%, 1.0% & 1.5% Standard Deviation for Voltage, Power Flow & Power Injection Measurements Respectively

	Integrated	Two-Level
$Macc_v$	0.0016 PU	0.0023 PU
$\|\|P_{error}\|\|_1$	0.4683 MW	0.9579 MW
$\|\|P_{error}\|\|_\infty$	0.06868 MW	0.0986 MW

Case 2: The meters are connected to the secondary of the current transformers (CT) and potential transformers (PT). Even though, one uses highly accurate digital meters, measurements are erroneous due to errors introduced by CTs and PTs. The errors added to the measurements in Case 1 are quite small for realistic studies. In this case, the measurements are added with random errors with zero mean and a standard deviation of 1.0% for voltage measurements, 1.5% for power flow measurements and 3.0% for power injection measurements. Table 2.3 shows the results obtained by integrated and two-level state estimators.

Table 2.3 SE Results with 1.0%, 1.5% & 3.0% Standard Deviation for Voltage, Power Flow & Power Injection Measurements Respectively

	Integrated	Two-Level
$Macc_v$	0.0020 PU	0.0025 PU
$\|\|P_{error}\|\|_1$	0.6066 MW	1.0504 MW
$\|\|P_{error}\|\|_\infty$	0.0991 MW	0.1120 MW

2.4.5 Simulation Results 1896-Bus Real World System

1896-bus system consists of 4 areas. Following is the brief description of the system.

- Total number of branches: 2832
- Total number of tie-lines: 60
- Total number of boundary buses: 85

Table 2.4 1896-Bus System Information

Area	Number of Buses	Number of Boundary Buses
1	759	19
2	376	29
3	492	19
4	269	18

Case 1: All the measurements used for state estimation are added with random errors with zero mean and a standard deviation of 0.5% for voltage measurements, 1.0% for power flow measurements and 1.5% for power injection measurements. Table 2.5 shows the results obtained by the integrated and two-level state estimators obtained for the same measurement set.

Table 2.5 SE Results with 0.5%, 1.0% & 1.5% Standard Deviation for Voltage, Power Flow & Power Injection Measurements Respectively

	Integrated	Two-Level
$Macc_v$	0.0022 PU	0.0023 PU
$\|\|P_{error}\|\|_1$	36.6056 MW	49.0618 MW
$\|\|P_{error}\|\|_\infty$	0.3502 MW	4.0476 MW

Case 2: The measurements are added with random errors with zero mean and a standard deviation of 1.0% for voltage measurements, 1.5% for power flow measurements and 3.0% for power injection measurements. Table 2.6 shows the results obtained by the integrated and two-level state estimators.

Table 2.6 SE Results with 1.0%, 1.5% & 3.0% Standard Deviation for Voltage, Power Flow & Power Injection Measurements Respectively

	Integrated	Two-Level
$Macc_v$	0.02138 PU	0.05505 PU
$\|\|P_{error}\|\|_1$	42.2460 MW	677.3479 MW
$\|\|P_{error}\|\|_\infty$	0.6593 MW	134.633 MW

2.4.6 Discussion

Simulation results of IEEE 30-bus system indicate that for both cases, the results of integrated and two-level state estimator are comparable. But the same is not true for 1896-bus system simulation results. Investigating for the source of error in two-level state estimator reveals that high MW mismatch is observed between the estimated and actual active power flow in some internal short or low impedance transmission lines connected

to the boundary buses in all areas. This is the reason for one norm and infinity norm of the estimation norm for active power flow being very high when using two-level state estimation. As we know the boundary bus states are re-estimated at the coordinator level in this algorithm. The small variation in boundary bus states from first level to second level, because of re-estimation, causes a high power mismatch in short or low impedance transmission lines. The transmission lines with active power flow mismatch of 10 MW or more is listed in table 2.7. The bus numbers which are shown in bold are the internal boundary buses of one of the four areas. The rest of the buses are internal buses of one of the four areas.

Table 2.7 Short or Low Impedance Transmission Lines with Active Power Flow Mismatch of 10 MW or More

From Bus	To Bus	Estimated Flow (MW)	Actual Flow (MW)	Absolute Mismatch (MW)	Resistance R (PU)	Reactance X (PU)
75	448	-4.6384	20.0420	24.6804	0.0001	0.0002
789	791	-80.0519	-131.887	51.8355	0.00009	0.0008
1028	1029	54.6807	14.7487	39.9319	0.00016	0.00129
1028	1030	25.1645	13.1397	12.0248	0.00051	0.00442
1221	**1466**	94.0353	-40.5984	134.633	0.00008	0.00043
1233	**1236**	570.350	554.0378	16.3121	0.00019	0.00496
1252	**1275**	1130.065	1119.530	10.5352	0.000143	0.00159
1629	1668	91.5297	128.1376	36.6078	0.00008	0.00073
1644	1645	11.1863	0.00	11.1863	0.00	0.0001
1236	1277	-113.95	-102.397	11.5532	0.00007	0.007

2.5 Application of PMU Measurements in Two-Level State Estimation

To increase the accuracy of the boundary bus states, especially to which the short transmission lines are connected, it is required to increase the measurement redundancy and to use the more accurate measurements. The measurements provided by phasor measurement units are more accurate compared to the conventional measurements. Table 2.8 shows the list of phasor measurement units that are assumed to exist in 1896-bus system. The measurements available from synchronized PMUs are assumed to have a standard deviation of 0.01%. Table 2.9 shows the results of integrated and two-level state estimators with the synchronized PMU measurements along with the conventional measurements. The conventional measurements are added with random errors with zero mean and standard deviations described in case 2.

Table 2.8 Available PMU Measurements on 1896-Bus System

	Bus Number	Location
1	667	Area 1 slack bus
2	1051	Area 2 slack bus
3	1227	Area 3 slack bus
4	1863	Area 4 slack bus
5	75	Area 1
6	789	Area 2
7	1028	Area 2
8	1466	Area 3
9	1236	Area 3
10	1275	Area 3
11	1629	Area 4
12	1644	Area 4

Table 2.9 SE Results with Synchronized PMU Measurements Incorporated in Measurement Set

	Integrated	Two-Level
$Macc_v$	0.0194 PU	0.0362 PU
$\|\|P_{error}\|\|_1$	39.786 MW	66.0645 MW
$\|\|P_{error}\|\|_\infty$	0.5680 MW	11.1863 MW

The results shown in table 2.9 indicate that the impact of synchronized phasor measurements on integrated state estimator is not very significant but it improves the results of two-level state estimator significantly, especially lowering the errors in short or low impedance transmission lines. PMU measurements are used in both levels of two-level state estimation. Because, PMU measurements are assumed to have an accuracy of 0.01%, both levels of state estimator gives very high weight to it. Hence, there is not significant variation in boundary bus state estimates from one level to another, which helps reducing the error in estimation of active power flow in low impedance or short transmission lines. The errors observed in two-level state estimator can be reduced further if PMU measurements can be made available from each boundary bus.

2.6 Effect of System Decomposition on TLSE

In this section, several two-level state estimation methods based on overlapped and non-overlapped system decomposition are presented and their performances are compared with the integrated state estimator. Depending on system decomposition, the state vector of central coordinator may include boundary bus states. Ideally, it is beneficial if the systems are overlapped, as it increases redundancy in boundary networks

and hence increases the accuracy of boundary bus states at the individual level. At the coordination level, it is important to re-estimate the boundary bus states as it allows detection of any bad measurement, which may have gone undetected at the individual level because of low redundancy. Hence, an overlapped system with re-estimation of boundary bus states at coordination level is an ideal option for wide area state estimator.

2.6.1 Non-Overlapped Systems

Consider an interconnected system with N areas shown in Fig. 2.5. Individual areas are connected to each other through the tie-line network. In this section, the areas are considered to be non-overlapping, i.e., Area 1 will restrict its model to buses A1-1 and A1-2. All the area follow similar scheme.

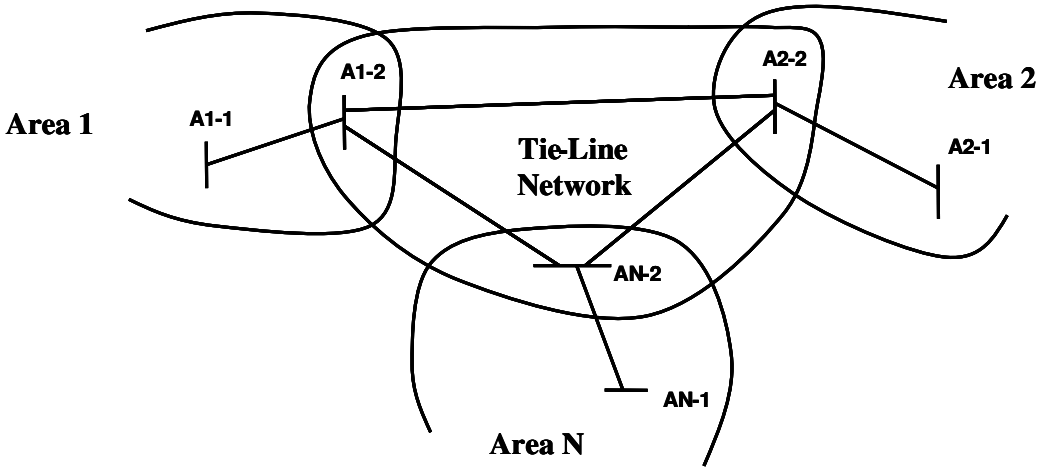

Figure 2.5: System Decomposition - Non-Overlapped Systems

The buses in each area can be categorized as internal buses and internal boundary buses. For example, in Area 1, A1-1 is internal bus and A1-2 is internal boundary bus. Based on system decomposition, the state vector for individual area 'i' can be written as

$$x_i^T = [x_i^{\text{int}}, x_{i,b}^{\text{int}}] \qquad (2.11)$$

where,

$\boldsymbol{x_i^{int}}$ internal bus states of the i^{th} area

$\boldsymbol{x_{i,b}^{int}}$ internal boundary bus states of the i^{th} area

Case 1: In this case, the boundary bus states are not re-estimated at the second stage of the algorithm but are used as the parameters. Hence the state vector of the central coordinator is defined as

$$x_C = [U^T] \qquad (2.12)$$

where,

$$U = [u_2, u_3, ..., u_N]^T$$

$\boldsymbol{u_i}$ is the phase angle of i^{th} area reference bus with respect to the global reference. Here, area 1 reference bus is arbitrarily chosen as the global reference bus. The measurement vector in this case includes only the tie-line flows.

Case 2: In this case, the boundary bus states of each area are re-estimated at the coordinator stage. Hence the state vector of the central coordinator is defined as

$$x_C = [U^T, x_b^T] \tag{2.13}$$

where,

$$U = [u_2, u_3, ..., u_N]^T$$

$$x_b = [x_{1,b}, x_{2,b}, ..., x_{N,b}]^T$$

The measurement vector in this case can be written as,

$$z_C = [z_b, \hat{x}_b^{\text{int}}] \tag{2.14}$$

where,

$$\hat{x}_b^{\text{int}} = [\hat{x}_{1,b}^{\text{int}}, \hat{x}_{2,b}^{\text{int}}, ..., \hat{x}_{N,b}^{\text{int}}]$$

z_b is the set of boundary measurements which may include tie-line power flows and voltage measurements of the boundary buses. The boundary bus states of each area from individual area state estimators are used as the pseudo measurements at the second level.

2.6.2 Overlapped Systems

Consider an interconnected system with N areas shown in Fig. 2.6, which is identical to the one shown in Fig. 2.3. Individual areas are considered to be overlapping

and the buses in each area can be categorized as internal buses, internal boundary buses and external boundary buses.

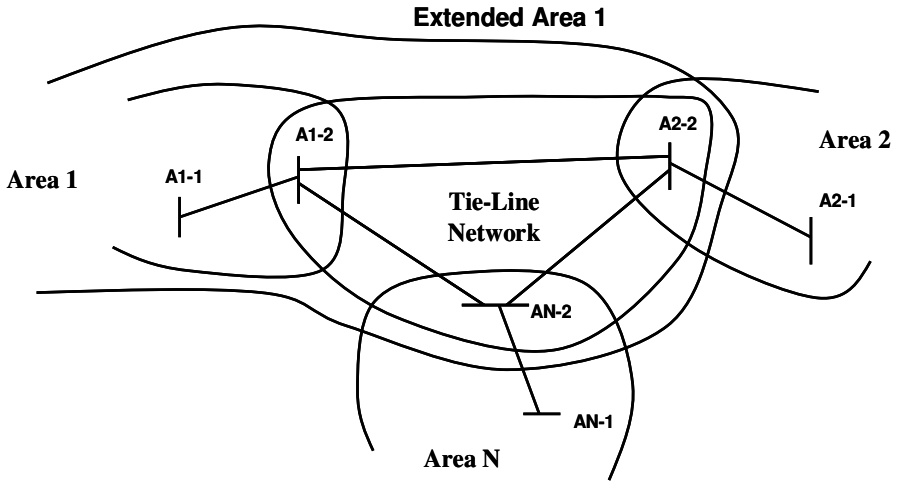

Figure 2.6: System Decomposition - Overlapped Systems

Based on system decomposition, the state vector for individual area 'i', at the first level, can be written as

$$x_i^T = [x_i^{\text{int}}, x_{i,b}^{\text{int}}, x_{i,b}^{ext}] \qquad (2.15)$$

where,

x_i^{int}	internal bus states of the i^{th} area
$x_{i,b}^{int}$	internal boundary bus states of the i^{th} area
$x_{i,b}^{ext}$	external boundary bus states of the i^{th} area

Case 3: As case 1, the boundary bus states are not re-estimated at the second level in this case, but are used as the parameters. Hence the state vector of the central coordinator is defined as

$$x_C = [U^T] \tag{2.16}$$

where,

$$U = [u_2, u_3, ..., u_N]^T$$

The measurement vector in this case includes only the tie-line flows.

Case 4: As Case 2, the boundary bus states of each area are re-estimated at the coordinator stage in this case. Hence the state vector of the central coordinator is defined as

$$x_C = [U^T, x_b^T] \tag{2.17}$$

where,

$$U = [u_2, u_3, ..., u_N]^T$$
$$x_b = [x_{1,b}, x_{2,b}, ..., x_{N,b}]^T$$

The measurement set available for the central coordinator is given as

$$z_C = [z_b, \hat{x}_b^{\text{int}}, \hat{x}_b^{ext}] \tag{2.18}$$

where,

$$\hat{x}_b^{\text{int}} = [\hat{x}_{1,b}^{\text{int}}, \hat{x}_{2,b}^{\text{int}}, ..., \hat{x}_{N,b}^{\text{int}}]$$
$$\hat{x}_b^{ext} = [\hat{x}_{1,b}^{ext}, \hat{x}_{2,b}^{ext}, ..., \hat{x}_{N,b}^{ext}]$$

The boundary bus states from individual area state estimator are used as pseudo-measurements at the coordinator level. In this case, it is possible that each boundary bus has two pseudo measurements, one from the area to which the bus is internal boundary bus and another from the area to which the bus is external boundary bus, which is usually the neighbor system.

2.6.3 Simulation Results 1896-Bus Real World System

All four algorithms are tested on a real world 1896 bus system, which consists of four areas. The results obtained are compared with the results obtained by integrated state estimator. All the measurements used for state estimation are added with random errors with zero mean and a standard deviation of 0.5% for voltage measurements, 1.0% for power flow measurements and 1.5% for power injection measurements. The power injection measurements at the boundary buses are not considered at the second level in any of the algorithm, as they requires to transfer the topology and line information of the internal transmission lines connected to the boundary buses. Table 2.10 summarizes the simulation results obtained on 1896-bus real world system.

Table 2.10 Simulation Results for 1896-Bus System

	ISE	Case 1	Case 2	Case 3	Case 4
$Macc_v$	0.0022 PU	0.0026 PU	0.0026 PU	0.0025 PU	0.0027 PU
$\|\|P_{error}\|\|_1$	36.60 MW	155.26 MW	213.99 MW	58.44 MW	116.07 MW
$\|\|P_{error}\|\|_\infty$	0.35 MW	24.77 MW	29.34 MW	2.80 MW	16.45 MW

The results indicate that case 3 gives the best results out of all four cases, compare to the integrated state estimator. Case 3 uses the overlapped system decomposition and do not re-estimate the boundary bus states at the co-ordination level. Cases 1 & 2, uses the non-overlapped system decomposition and shows much higher error compared to the integrated state estimation. Case 3 gives the best results; however, because it does not re-estimate the boundary bus states at the co-ordination level, it is not possible to detect any bad data present in the measurement set, which may have gone undetected in the first level because of low redundancy or criticality. Hence, it is necessary to re-estimate the boundary bus states at the co-ordination level, which makes case 4 more favorable. To improve the accuracy of results of case 4, it is important to use boundary injection measurements at coordination level. The simulation results presented in previous and this section reveals that it is important to use overlapped systems and to re-estimate boundary bus states at second level. It is also observed that the performance of two-level state estimator can be significantly increased by using boundary injection measurements at second level.

2.7 Conclusion

This chapter investigates the two-level state estimation algorithm for a multi-area interconnected power system. The traditional state estimator is not suitable for multi-area network because it requires a large amount of real-time data exchange between utilities. The utilities are reluctant to share real-time data because of confidentiality and security reasons. The two-level state estimator requires the individual areas to share their state

estimator results only to the central coordinator, who will coordinate and bring them to a global reference. In this chapter, a scheme is proposed which can utilize the boundary injection measurements at the second level without exchanging the topology data of internal transmission lines connected to boundary buses. The use of synchronized phasor measurements is justified and implemented to increase the accuracy of the two-level state estimator. Simulation results obtained for the IEEE 30-bus system and 1896-bus real world system shows that fast and accurate wide area state estimation is possible using two-level state estimation approach. This chapter also presents the effect of system decomposition on the performance of two-level states estimator and discusses pros and cons of each.

CHAPTER THREE

AVAILABLE TRANSFER CAPABILITY

This chapter presents a new iterative method to calculate Available transfer capability (ATC) of power system. Available transfer capability is the additional power that can be transferred between two nodes of the system without hitting thermal, voltage and transient stability limits. Existing linear ATC calculation methods are either based on DC or AC Power Transfer Distribution Factors (PTDFs). These methods are fast but do not consider control changes such as generator reactive limits and bus voltage limits while calculating ATC. Optimal Power Flow (OPF) and Continuation Power Flow (CPF) can produce accurate ATC values but can be very time consuming and cannot be used in real-time operations environment. The method proposed in this chapter aims to overcome all these dis-advantages. It does not require repeated solution of power flow and also considers the control changes of the system with the increase in transfer limit.

3.1 Available Transfer Capability

In 1996, since Federal Energy Regulatory Commission (FERC) provided open access of the transmission network to utilities, large scale power transactions between utilities have increased in order to provide reliable and economical electric supply. For example, hydroelectric power generated in Canada can be transferred to consumers and industry in Los Angeles using the high voltage transmission system. In large interconnected power networks, there may be multiple control areas with system operators responsible for different areas. The system operators must have some procedure

for exchanging information and making decisions that affect the patterns of use across grid. With the competitive market, system operators face the need to monitor and coordinate power transactions taking place over long distances in different areas. In such situations, system operators need answer to a question, "How much power can be transmitted reliably between two buses of an interconnected system?" Available transfer capability and Total Transfer Capability (TTC) can provide system operators useful information regarding the total power transfer possible between two nodes without hindering the reliability of the system.

The Federal Energy Regulatory Commission requires that the available transfer capability information should be made available on a publicly accessible Open Access Information Sharing System (OAISS) on the real-time basis [12]. ATC is defined as a measure of the transfer capability, in the physical transmission network, for transfers of power over and above already committed uses. According to North American Electric Reliability Corporation's (NERC) definition, total transfer capability indicates the amount of power that can be transferred between two buses in the system in a reliable manner in a given time frame [12-13]. The total transfer capability is the largest flow for which there are no thermal overloads, voltage limit violations, voltage collapse and/or any other system security problems such as transient stability. The ATC can be defined as "A measure of transfer capability in the physical transmission network for further commercial activity over and above already committed uses". This definition can be formulated as following equation,

ATC = TTC – CBM – TRM – "Existing Transmission Commitments"

Where,

CBM: Capacity Benefit Margin

TRM: Transmission Reliability Margin

The ATC problem is the determination of the largest additional amount of power above some base case value that can be transferred in a prescribed manner between two sets of buses: the source, in which power injections are increased, and the sink, in which power injections are decreased by same amount. Increasing the power transfer, increases the loading in the network and at some point causes an operational or physical limit to be reached that prevents further increase. The largest value of power transfer that causes no limit violations, with or without a contingency, is used to compute the ATC. The problem can be formulated as:

$$Maximize\ J = f(x,u) \tag{3.1}$$

Subject to,

$$g(x,u) = 0$$

$$h^{\min} \le h(x,u) \le h^{\max}$$

Where, u and x are the control and state vectors respectively. $g(x,u)$ is the power flow equality constraints shown in equation (3.2).

$$P_i - V_i \sum_{j=1}^{N} V_j (G_{ij} \cos\theta_{ij} + B_{ij} \sin\theta_{ij}) = 0$$
$$Q_i - V_i \sum_{j=1}^{N} V_j (G_{ij} \sin\theta_{ij} - B_{ij} \cos\theta_{ij}) = 0 \qquad (3.2)$$

Where, P_i & Q_i are net active and reactive power injections at bus 'i'. $V_i \angle \theta_i$ is the voltage at bus 'i' and ($G_{ij} + j\, B_{ij}$) is corresponding element from bus admittance matrix.

h(x,u) is the inequality constraint function and is shown in equation (3.3).

$$\begin{aligned} P_{Gi}^{\min} &\le P_{Gi} \le P_{Gi}^{\max} && i \in R \\ Q_{Gi}^{\min} &\le Q_{Gi} \le Q_{Gi}^{\max} && i \in R \\ V_i^{\min} &\le V_i \le V_i^{\max} && i \in S \\ 0 &\le P_l \le P_l^{\max} && l \in T \end{aligned} \qquad (3.3)$$

where,
R: set of all generator buses
S: set of all buses in system
T: set of all transmission lines of system

3.2 Methods to Calculate ATC

There are three basic methods that can be used for transfer capability calculations. The fastest method is based on DC load flow model and it uses linear power transfer distribution factors to determine transfer capability in the system [14-15, 34]. The fact that distribution factors are easy to calculate and can give quickly rough figures of transfer capability made them attractive. Since those factors are based on DC load flow ignoring voltage and reactive power effects as well as system nonlinearity, they might

lead to unacceptable error especially in a stressed system with insufficient reactive power support and voltage control. Still PTDF can be used to update transfer capability in some systems where voltage problems are not pronounced [14]. Recently a use of AC power transfer distribution factors for transfer capability calculation is investigated [35, 36]. Generally, AC-PTDFs are derived at base case load flow result. They are also easy and quick to calculate transfer capability of the network. However, the results are not as accurate as repeated power flow. These limitations of using DC/AC-PTDFs in computing transfer capability can be avoided by using the Repeated Power Flow (RPF) [37].

Another popular approach for transfer capability calculation is the continuation power flow [38-41]. From the solved base case, power flow solutions are sought for increasing amounts of transfer in the specified direction. The quantity of the transfer is a scalar parameter which can be varied in the model. The amount of transfer is gradually increased from the base case until a binding limit is encountered. This continuation process requires a series of power flow solutions to be solved and tested for limits. Because CPF considers system non-linearity and voltage-reactive power aspects, the transfer capability results are significantly accurate. But it ignores optimal distribution of generation and loading and hence may lead to a conservative transfer value. Also, system reactive power optimization and voltage control are usually not considered in CPF, which might have significant impacts on system transfer capability.

The last approach recently used for transfer capability calculations is optimal power flow. OPF has been investigated extensively in the past three decades [18-19].

OPF techniques are quite mature and have recently found some applications in transfer capability studies [42, 43]. All of these works share the common theme that they formulate an optimization problem in which the dominant elements are the equality constraints arising from the power flow. OPF methods can also play an important role in the current deregulated environment as it has the potential to distribute the resources optimally. Furthermore, OPF can model the system constraints including ac load flow equations, transmission line thermal limits and voltage limits in both transfer capability and economic dispatch studies.

Studies have indicated that CPF and OPF are accurate methods for transfer capability calculations but they are very time consuming. It is almost impossible to justify the use of CPF and OPF based methods for transfer capability calculations in real-time. For example, if we want to calculate ATC by incrementing the transfer, resolving the power flow and iterating in that manner and if it takes 10 iterations to calculate ATC and there are 600 contingencies to be considered, we have 6000 power flows to solve. If it takes 30 seconds to solve a power flow, which is a reasonable guess, then it will take 50 hours to obtain ATC value for each contingency. In case of OPF, it may take anywhere from few minutes to an hour to obtain the solution of one power flow. Hence, CPF and OPF are good methods for off-line use for planning. In today's deregulated power system, we need a ATC calculation method which is fast and accurate and can also be applied for multi-area ATC calculations. This chapter presents a new iterative ATC calculation method, which does not require a solution of power flow repeatedly and is more accurate compared to using DC/AC-PTDF to calculate ATC.

3.3 Power Transfer Distribution Factors

3.3.1 DC - Power Transfer Distribution Factors

The problem of studying thousands of possible power transfers and outages becomes very difficult to solve if it is required to present results quickly. One of the easiest ways to provide a quick calculation is to use linear sensitivity factors or DC-PTDFs. These factors show the approximate change in line flows for changes in generation on the network and are derived from DC load flow. Consider a bus *m* and a line joining buses *i* and *j*.

$$PTDF_{ij,m} = \frac{\Delta P_{ij}}{\Delta P_m} \qquad (3.4)$$

where,

ΔP_{ij} = change in real power flow on line *ij* for a change of ΔP_m occurs at bus *m*.

ΔP_m = change in generation at bus *m*.

The PTDF from injection at bus *m* to flow over the transmission line connecting bus *i* and bus *j* is written as

$$PTDF_{ij,m} = \frac{X_{im} - X_{jm}}{x_{ij}} \qquad (3.5)$$

Where, x_{ij} is the reactance of the transmission line connecting bus *i* and bus *j*; X_{im} and X_{jm} are the elements of bus reactance matrix.

From the power flow point of view, a transaction is a specific amount of power that is injected into the system at one bus *m* by a generator and removed at another bus by a load at another bus *n*. In this case, the PTDF for injection at bus *m* and withdrawal at bus *n* to flow on the line connecting bus *i* and bus *j* can be written as

$$PTDF_{ij,mn} = \frac{X_{im} - X_{jm} - X_{in} + X_{jn}}{x_{ij}} \qquad (3.6)$$

ATC is limited by the maximum power flow of any one transmission line of the system. To determine the ATC it is necessary to compute the maximum power transfer, $T_{l,mn}$ for each line of the system in turn assuming it is the limiting line.

$$T_{l,mn} = \frac{Max_l - P_l}{PTDF_{l,mn}} \qquad (3.7)$$

The smallest $T_{l,mn}$ identifies the most constraining branch and thus gives the maximum power transfer. Hence, ATC can be written as

$$ATC = \min\{T_{l,mn}\} \qquad (3.8)$$

3.3.2 AC - Power Transfer Distribution Factors

The linear DC power transfer distribution factors based on DC power flow method are widely used to allocate MW flows on the lines for a transaction in the system. However, because they are only depended on topology of the system, they do not produce accurate results. For accurate AC analysis, one needs a PTDF which is also based on an operating point of the system in addition to system topology. [47-48] presents such AC-PTDFs, which are derived from a Jacobin matrix of an operating point load flow. Consider that the base case load flow result at the operating point is available; hence the Jacobin matrix can be written as

$$\begin{bmatrix} \Delta\delta \\ \Delta V \end{bmatrix} = [J_0]^{-1} \begin{bmatrix} \Delta P \\ \Delta Q \end{bmatrix} \tag{3.9}$$

Now for a given transaction of ΔT MW between seller bus 'm' and buyer bus 'n', only following two entries in the mismatch vector of RHS of the above equation will be non-zero.

$$\Delta P_m = \Delta T; \quad \Delta P_n = -\Delta T;$$

With the above mismatch vector elements, the change in voltage angle and magnitude at all the buses can be computed and hence the new voltage profile can be calculated. The new line flows can be calculated using new voltage profile and also the change in line flows. Once the change in line flows is calculated for a given transaction of ΔT, AC-PTDFs can be obtained using following equation.

$$PTDF_{ij,mn} = \frac{\Delta P_{ij}}{\Delta T} \qquad (3.10)$$

These AC-PTDFs, which are computed at a base case operating point, can be used to calculate ATC for a given transaction as explained using DC-PTDFs. The basic steps used to calculate AC-PTDF for a given transaction are summarized below:

- Run a base case load flow
- Form a full Jacobin to include all buses except the slack bus and invert it.
- For each transaction,
    - Identify the selling bus and buying bus
    - Assume positive injection change at selling bus and negative injection change at buying bus
    - Compute the change in voltage magnitudes and angles and update the voltages
    - Calculate new transmission line flows and hence the AC-PTDFs.

AC-PTDFs are quite accurate in modeling the impact of contingencies and power transfers. However, they only use derivatives around the present operating point. Thus, control changes as you ramp out to the transfer limit are not modeled. The possibility of generators participating in the transfer hitting limits is not modeled.

3.4 Iterative Method for ATC Calculation

Among the existing methods of ATC calculations, PTDF based method is fastest. But DC-PTDFs are depended only on system topology and AC-PTDFs uses derivatives around the operating point only. Control changes are not modeled when using either PTDFs as you ramp out to the transfer limit. Hence, using PTDFs for ATC calculations do not produce accurate results. Studies have indicated that CPF and OPF are accurate methods for determining transfer capability calculations but they are very time consuming. It is almost impossible to justify the use of CPF and OPF based methods for ATC calculations in real-time.

The proposed iterative method for ATC calculation overcomes disadvantages of existing methods and can be used in real-time. The main characteristics of the proposed method are:

- It is based on current operating state of the system.
- It does not require sequential power flow solution and hence is faster than OPF and CPF based methods.
- It takes into account generator limits and bus voltage limits in addition to transmission line thermal limits, which are usually neglected in PTDF based methods.

The proposed method uses the base case load flow solution and the sensitivity properties of the Newton-Raphson Load Flow (NRLF) Jacobin matrix. NRLF involves iterative solution of linear equations, with the state vector computed and updated in each

iteration for a small change in power injections. The linear equation is shown is equation (3.11).

$$\begin{bmatrix} \Delta\delta \\ \Delta V \end{bmatrix} = \left[J_0\right]^{-1} \begin{bmatrix} \Delta P \\ \Delta Q \end{bmatrix} \qquad (3.11)$$

The iterative procedure stops when the change in the state vector between successive iterations is smaller than a specified value. Thus the Jacobin calculated after the last load flow run is available for use. The proposed method uses the Jacobin obtained at base case load flow to calculate the change in voltage magnitudes and angles for a power transaction between two buses. The transaction amount is kept small to keep the iterative solution accurate. Thus, for the specific transfer, only two entries are non-zero in the RHS vector of the equation (3.11). After the change in voltage magnitudes and angles is obtained, they are superimposed on the base case complex voltages, to obtain new complex voltages. Linearization over such a small interval does not introduce significant amount of error and hence the computation of complex bus voltages is feasible and accurate. New bus voltages are compared with their respective limits and if they are not violated, new transmission line flows, bus injections and generator quantities are calculated. These quantities are then compared with their respective limits. If none of the limits are violated then the new Jacobin is calculated at the current state and the transaction is increased by small amount to repeat the above procedure. The procedure is repeated until at least either of transmission line thermal limit, generator limit or voltage limit is not violated. Figure (3.1) shows the flowchart of proposed method. The method

assumes that system has large dynamic stability margin and the bus voltage limit is reached before system loses voltage stability.

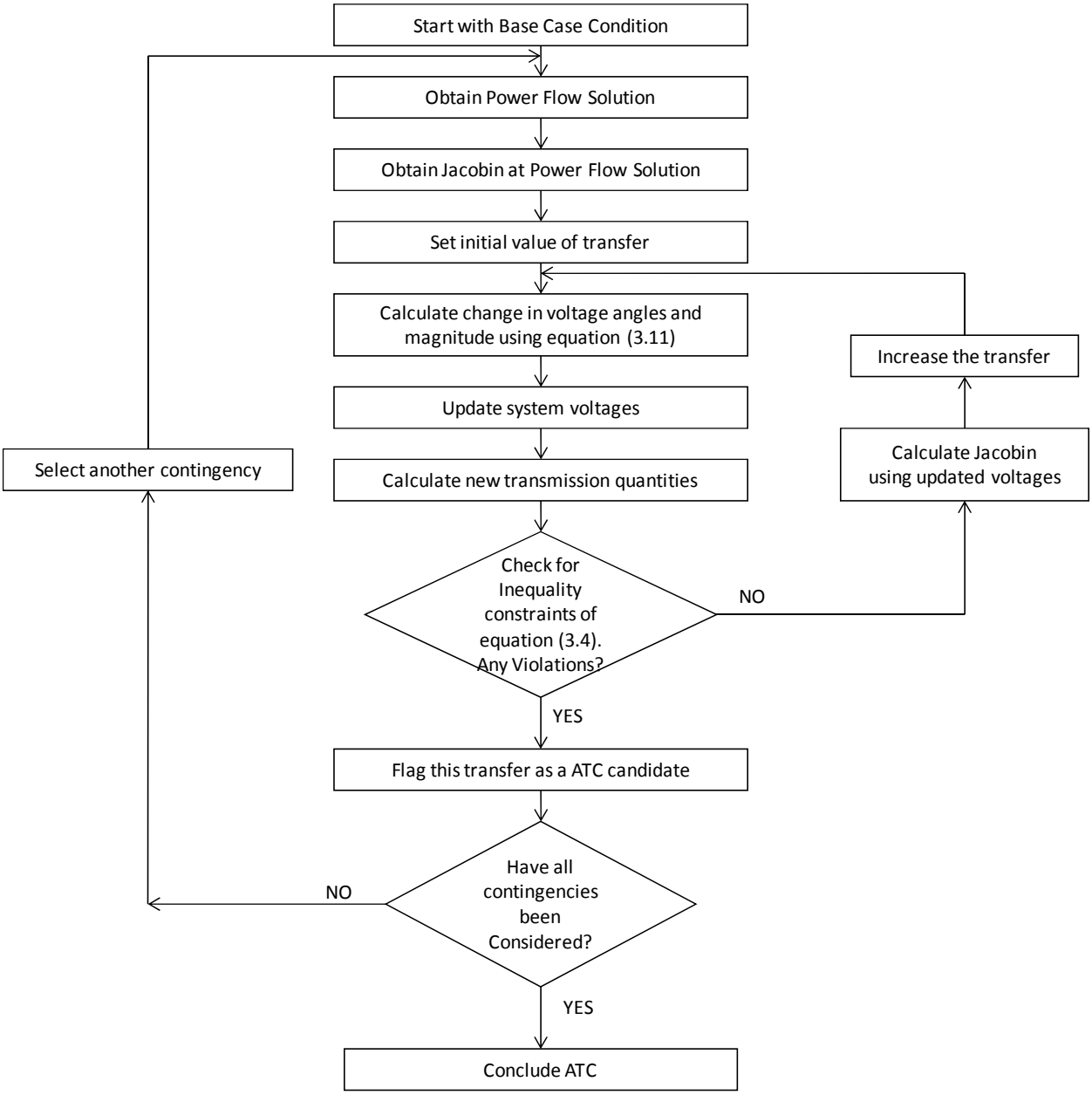

Figure 3.1: Flowchart of proposed method

3.5 Simulation Results

The proposed method is tested on IEEE 6-bus and 39-bus systems. ATC values are presented for two power transactions for each system and it is assumed that only two contingencies are present in the contingency list to consider. Results are also presented at 80% and 120% of base case loading for each system. ATC results obtained using the proposed method is compared with the results obtained using DC-PTDFs, AC-PTDFs and repeated AC Load Flow (ACLF).

3.5.1 IEEE 6-Bus System

ATC results for power transactions between buses 2-3 and 1-5 are presented in Table 3.1 and 3.2 respectively. For the transfer from bus 2 to bus 3, in base case condition, line 2-3 reaches the limit for a transfer of 214.50 MW. This is the actual ATC value as it is calculated using repeated ACLF. The ATC value calculated using DC and AC PTDFs is 245.50 MW and 225.04 MW, which represents 14.5% and 4.91% error respectively. ATC amount calculated using proposed method is 215.75 MW, which is comparable with actual ATC amount. The same can be concluded for a power transfer from bus 1 to bus 5. The proposed method predicts same limiting factor as predicted by repeated ACLF method for both transactions. The limiting factors predicted by PTDFs based methods are not same as predicted by proposed or ACLF based method, especially for the transfer from bus 2 to 3.

Table 3.1: ATC for transfer from Bus 2 to 3

	DCPTDF based method		ACPTDF based method		Proposed Method		Repeated ACLF Method	
	ATC (MW)	Limiting Factor	ATC (MW)	Limiting Factor	ATC (MW)	Limiting Factor	ATC (MW)	Limiting Factor
Base Case	245.50	Line 2-3	225.04	Line 2-3	215.75	Line 2-3	214.50	Line 2-3
Line 1-5 out	210.10	Line 2-6	197.46	Line 2-6	188.75	Line 2-3	188.00	Line 2-3
Line 2-6 out	160.70	Line 2-3	139.76	Line 2-3	135.50	Line 2-3	134.50	Line 2-3

Table 3.2: ATC for transfer from Bus 1 to 5

	DCPTDF based method		ACPTDF based method		Proposed Method		Repeated ACLF Method	
	ATC (MW)	Limiting Factor	ATC (MW)	Limiting Factor	ATC (MW)	Limiting Factor	ATC (MW)	Limiting Factor
Base Case	164.30	Line 1-5	146.39	Line 1-5	141.50	Line 1-5	140.50	Line 1-5
Line 1-5 out	94.70	Line 1-4	72.71	Line 1-4	66.25	Line 1-4	66.50	Line 1-4
Line 2-6 out	147.50	Line 1-5	132.21	Line 1-5	124.75	Line 1-5	125.10	Line 1-5

Table 3.3: ATC (MW) for transfer from Bus 2 to 3
at different loading conditions

% of Base Case	AC-PTDF based method	Proposed method	Repeated ACLF method
80	238.41	219.00	218.00
100	225.04	215.75	214.50
120	200.52	185.50	184.00

Table 3.3 shows the ATC values calculated at 80%, 100% and 120% of base case loading. AC-PTDFs used to calculate ATC are obtained at 100% of base case loading. Results shown in Table 3.3 indicates that error introduced in ATC values calculated by AC-PTDFs at 80% and 120% of base case loading is higher compared to error observed for 100% of base case loading. Proposed method does predict ATC value very close to one obtained using repeated ACLF regardless of the operating point.

3.5.2 IEEE 39-bus system

ATC results for power transactions between buses 32-39 and 36-38 are presented in Tables 3.4 and 3.5 respectively. The results indicate that ATC value calculated using proposed method closely matches with the one calculated using repeated AC load flow method and both methods also predict the same limiting factor. It is important to note that in few cases presented here, DC and AC-PTDFs based methods do not predict the same limiting factor as predicted by proposed or repeated ACLF method.

Table 3.4: ATC for transfer from Bus 32 to 39

	DC-PTDF based method		AC-PTDF based method		Proposed Method		Repeated ACLF Method	
	ATC (MW)	Limiting Factor	ATC (MW)	Limiting Factor	ATC (MW)	Limiting Factor	ATC (MW)	Limiting Factor
Base Case	200.49	Line 6-11	239.09	Line 6-11	231.50	Line 6-11	230.50	Line 6-11
Line 5-6 out	327.40	Line 4-14	286.24	Line 13-14	278.50	Line 13-14	277.50	Line 13-14
Line 17-18 out	151.38	Line 6-11	192.96	Line 6-11	184.00	Line 6-11	184.00	Line 6-11

Table 3.5: ATC for transfer from Bus 36 to 38

	DC-PTDF based method		AC-PTDF based method		Proposed Method		Repeated ACLF Method	
	ATC (MW)	Limiting Factor	ATC (MW)	Limiting Factor	ATC (MW)	Limiting Factor	ATC (MW)	Limiting Factor
Base Case	472.75	Line 16-17	512.55	Line 16-17	493.75	Line 16-17	495.00	Line 16-17
Line 5-6 out	437.57	Line 16-17	488.34	Line 16-17	465.50	Line 16-17	465.10	Line 16-17
Line 17-18 out	495.80	Line 16-17	541.04	Line 23-24	525.75	V_{24} Limit	525.50	V_{24} Limit

Table 3.6 represents the ATC amounts at new operating points with -20% and +20% variation of generation and load at each bus. AC-PTDFs method uses the PTDFs calculated at base case to calculate ATC at new operating points. Results indicate that error observed in ATC value calculated by AC-PTDFs is higher for 80% and 120% of base case loading compared to at 100% base case loading. Results also indicate that there is no effect of system loading condition on ATC values calculated by proposed method as they are comparable with the one obtained using repeated ACLF.

Table 3.6: ATC (MW) for transfer from Bus 32 to 39
at different loading conditions

% of Base Case	AC-PTDF based method	Proposed method	Repeated ACLF method
80	346.18	342.50	344.00
100	239.09	231.50	230.50
120	132.01	123.25	122.80

3.6 Conclusion

This chapter proposed a new iterative method for ATC calculation. The DC-PTDFs based method for ATC calculation is fast but do not produce accurate results as it is only based on system topology. AC-PTDFs based method for ATC calculation is also fast but it does not take into account generator limits and bus voltage limits. OPF and CPF based methods are accurate but they are very time consuming and cannot be used in real-time. This chapter introduced a new iterative method, which does not require a repeated solution of power flow and also takes into account generator limits and bus voltage limits. Because it doesn't require a solution of repeated power flow, it can be used in real-time in control center to calculate ATC.

CHAPTER FOUR

MULTI-AREA TRANSFER CAPABILITY

Nowadays, utilities are transferring power over long distances to provide reliable and economical electricity to their customers. In such situations, utilities are required to evaluate the reliability and security of an interconnected system on multi-area basis. Calculation of Available Transfer Capability (ATC) is one of the few important factors used to evaluate static security of the system before committing to transfer power between two nodes of the system. This chapter presents a two-level approach to calculate ATC of a multi-area interconnected power system. The basic idea of the proposed method consists of exchanging just enough data so that each area can evaluate the ATC for given transfer between any two nodes of the system considering limiting factors of their own area. The central coordinator coordinates the ATC results obtained by each area to calculate ATC of an interconnected system.

4.1 Problem Definition

In today's interconnected power system, calculation of ATC has become very challenging for the transfers taking place all over the interconnection. A multi-area interconnected power system is shown in figure 4.1. Let us adopt the view point of area 1. When area 1 runs the ATC calculation for a transfer within its network, the results are based on the limiting factors from its own area. Area 1 will not consider limiting factors of neighbor utilities. But it is possible that for a transfer within area 1, an element such as

transmission line, transformer etc. of neighbor system is reaching its threshold. For a case with transfer between areas, it becomes difficult to calculate ATC if each participating area don't have complete model of each others system and of areas via whom the actual transfer is going to take place. For example, power transfer from area 1 to area 4 of a system shown in figure 4.1 takes place through area 2 and area 3. In such situation, entity calculating ATC should have complete model of all four areas. The ideal solution to this problem is to share complete real-time model and allow each area to run ATC using the complete model of an interconnected system. However, this solution is technically expensive if not impossible and hindered by confidentiality issues.

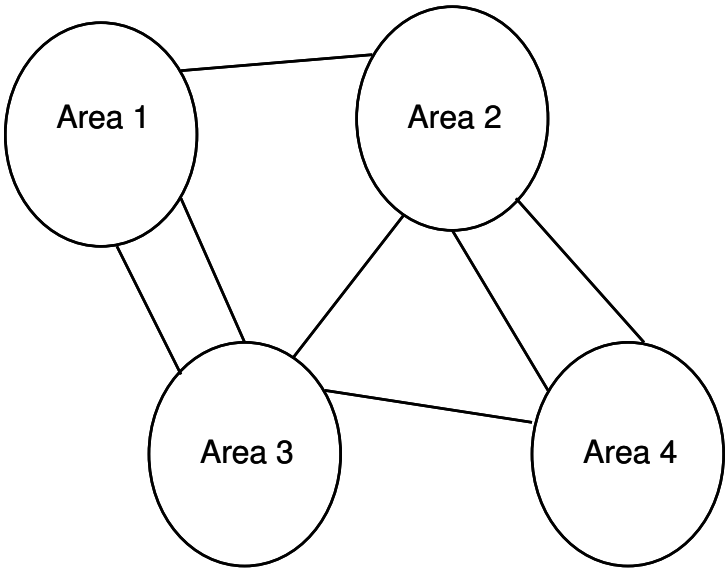

Figure 4.1: Multi-Area Interconnected Power System

An alternative method is based on a two-level multi-area coordinated solution which is similar to one used to achieve wide area state estimation. The main idea is to distribute the computations into individual areas and then coordinate their solutions in

order to reach the system-wide solution. The objective is to compute an ATC value, which is very close to the ATC that would be calculated if the entire system information was available to a single central operator. Such a two-level hierarchical approach for calculating ATC for interconnected power system is presented in [44-45] and is based on power transfer distribution factors. In [46], Bender decomposition is used to calculate the ATC, where the base case security constraints are treated as the high level problem. Two-level approach based on continuation power flow is presented in [47], which requires updating continuation parameter to ensure synchronized calculation in each area.

4.2 Equivalent Model of Neighbor Systems

In a multi-area system, it is assumed that each area operates autonomously by its own independent operator. Each area carries out its own ATC calculation and maintains its own detailed system model. To set up a base case operating point for ATC calculation, each area needs the model of neighbor systems. A theoretical solution to this problem is to use the complete real-time model of an interconnected system to calculate ATC. This is not possible because utilities are reluctant to share their real-time data due to security and confidentiality issues. The objective of the proposed framework is to rely on the exchange of minimal amount of information, while still achieving the above requirements. Therefore, instead of using detailed model requiring detailed data exchange, why not use the equivalent model? For the purpose of static security assessment, an equivalent model of an area is a black-box model of the voltage-current relationship at the receiving ends of the interconnections of that area, which can be

plugged into a power flow computation. Hence, each area uses network equivalents to represent the system in other areas except for the boundary buses, the seller bus and the buyer bus whose identities are maintained by excluding them from the equivalents. A two area interconnected system is shown in figure 4.2 as an example. From a view point of area 1, the system can be divided into three parts: 1) internal system; 2) boundary network, which includes boundary buses of internal and external system and tie-lines connecting them; and 3) external system. Considering area 1 operation, the external system excluding the boundary buses to which the tie-lines to area 1 are connected needs to be reduced to equivalent model.

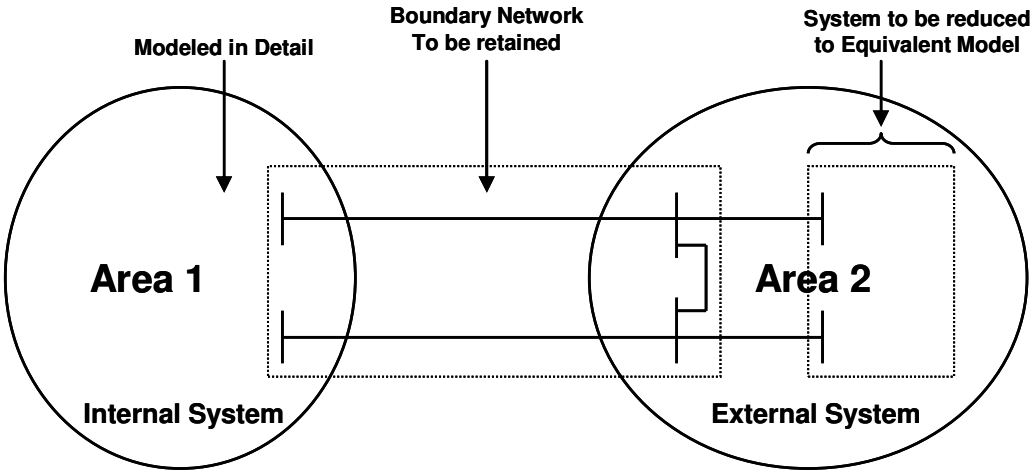

Figure 4.2: Two Area System

Among many equivalent techniques that appeared in the literature [48], Radial Equivalent Independent (REI) type equivalent is chosen here. REI-type equivalents are developed by Dimo [49], and later introduced to the U.S by Tinney and Powell in [50]. In

general, the REI network is a lossless network representation of a set of base case injections. The REI equivalent aggregates the injections of a group of buses into a single bus and distributes it into the system via a radial network. The key benefits of REI type equivalents are mentioned below.

1. The ability to eliminate all physical nodes, expect those which are the terminal nodes of the tie-lines or other key transmission lines whose identity is to be retained.
2. The generation and load buses are represented in an aggregate from by REI equivalents.
3. The reactive power can be provided by the equivalents more accurately especially around the base case operation.

The procedure of obtaining an REI equivalent shown in figure 4.3 is as follows:

1. The net complex power injection S_R can be presented as

$$S_R = \sum_{i=1}^{N} S_i$$

2. The voltage V_R must then be

$$V_R = \frac{S_R}{\sum_{i=1}^{N} (S_i / V_i)}$$

3. Dimo always assumed the voltage $V_G = 0$. So the branch admittances are

$$Y_i = \frac{-S_i^*}{|V_i|^2}, \qquad i = 1,...,N$$

$$Y_R = \frac{S_R^*}{|V_R|^2}$$

4. The final step in the process is to eliminate buses 1, 2, . . . , N and bus G by Kron reduction and obtain the equivalent network model.

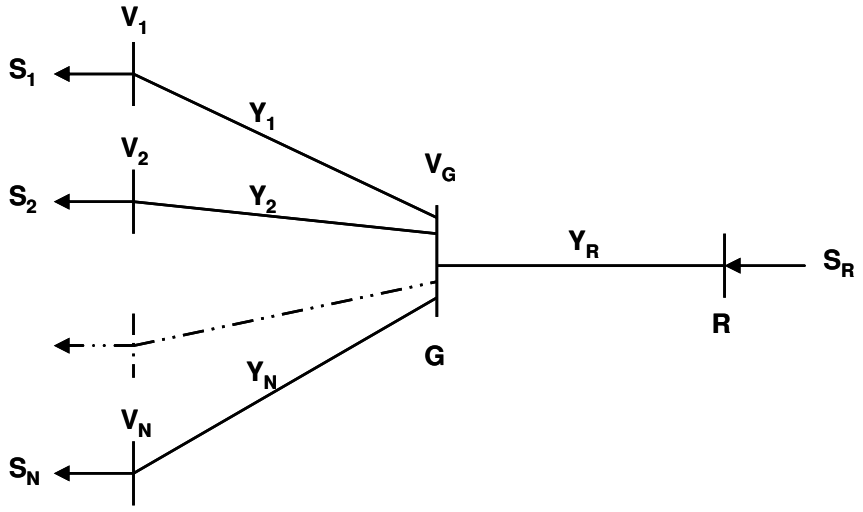

Figure 4.3: REI Network Configuration

Figure 4.4 represents the REI equivalent of area 2 connected to area 1. Savulescu [51] presented the use of REI equivalents for security analysis of power systems. Oatts et

al [52] presented the application of REI equivalents in operations planning to study the impact of scheduled interchanges on the system.

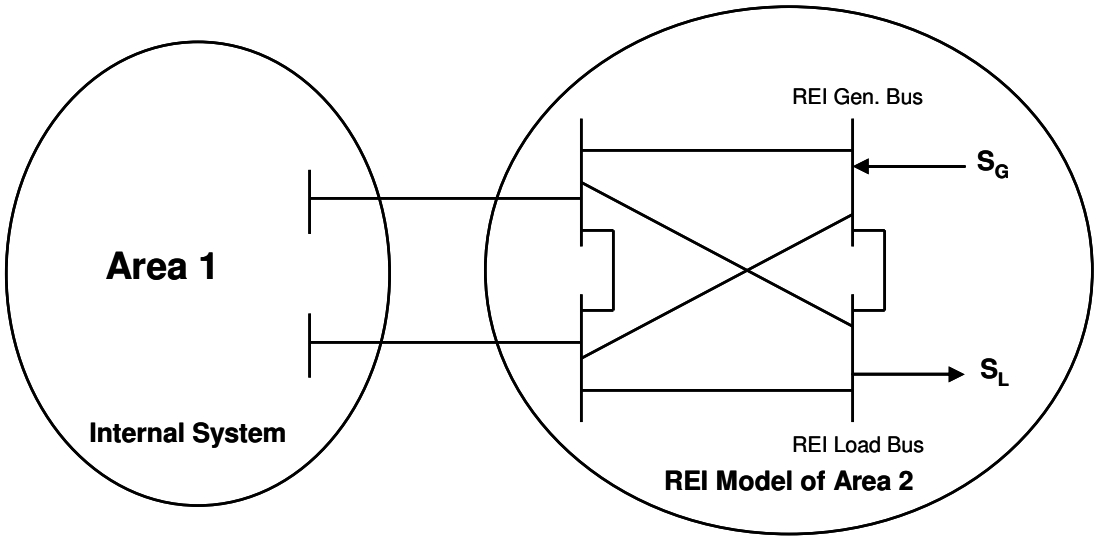

Figure 4.4: Area 2 presented by REI equivalent

4.3 Multi-Area ATC Calculation

The proposed two-level model assumes that each area calculates the ATC for a given power transaction by itself. In this process it uses the REI equivalent of neighbor utilities obtained from central coordinator to set up an operating case. Each area then sends the results to central coordinator, who coordinates them together and selects the minimum value of ATC for a given transaction, which is the ATC between buyer and seller bus with violating any thermal or voltage limits in any area of an interconnected power system. If buying or selling bus falls into particular area, it can not be reduced in

equivalent for use by other areas. Following is the summary of functions performed by central coordinator and individual areas respectively.

- Central Coordinator
  - Makes the list of transactions to be studied and sends them to participating areas.
  - Receives REI Equivalent from each area and re-distributes it to neighbor areas.
  - Compares the value of ATC obtained from each area and finds the smallest one. This is the ATC value for that transaction of an interconnected system. Central coordinator informs participating areas with ATC results.
- Each Control Area
  - Provides REI equivalent of own system to central coordinator.
  - Receives REI equivalent of neighbor systems from central coordinator and list of transactions to be studied.
  - Calculates ATC between the specified buyer and seller buses and sends the results to central coordinator.

Following is the sequence of work performed by central coordinator and each participating area.

1. Central coordinator distributes the list of transactions to be studied to participating areas.
2. Each area sends its equivalent model to central coordinator.
3. Each area receives equivalent models of their neighbor systems from central coordinator.
4. Each area calculates ATC for a list of transactions considering limiting factors of its own system and sends them to central coordinator.
5. Central coordinator compares the value of ATC obtained from each area and finds the smallest one. This is the ATC of an interconnected system which is sent back to each participating areas.

4.4 Simulation Results

The proposed two-level multi-area ATC calculation method is implemented on IEEE 39-bus system. This system is divided into three areas as shown in figure 4.5. The base case of the IEEE 39-bus system is used as the reference loading. Table 4.1 presents ATC values for transfer from bus 39 to bus 15. Area 1 calculates that 393MW of additional power can be transferred from bus 39 to bus 15 before hitting the thermal limit of line from bus 2 to 3. The limiting constraints for Area 2 and Area 3 are lines from bus 2 to 3 and bus 14 to 15 for an ATC of 1075MW and 653MW respectively. The coordinator selects the smallest transfer amount, which is 393MW as a multi-area ATC solution. The results obtained using integrated and multi-area solutions are comparable. It

is important to note that the limiting factors predicted by integrated and multi-area solutions are also same.

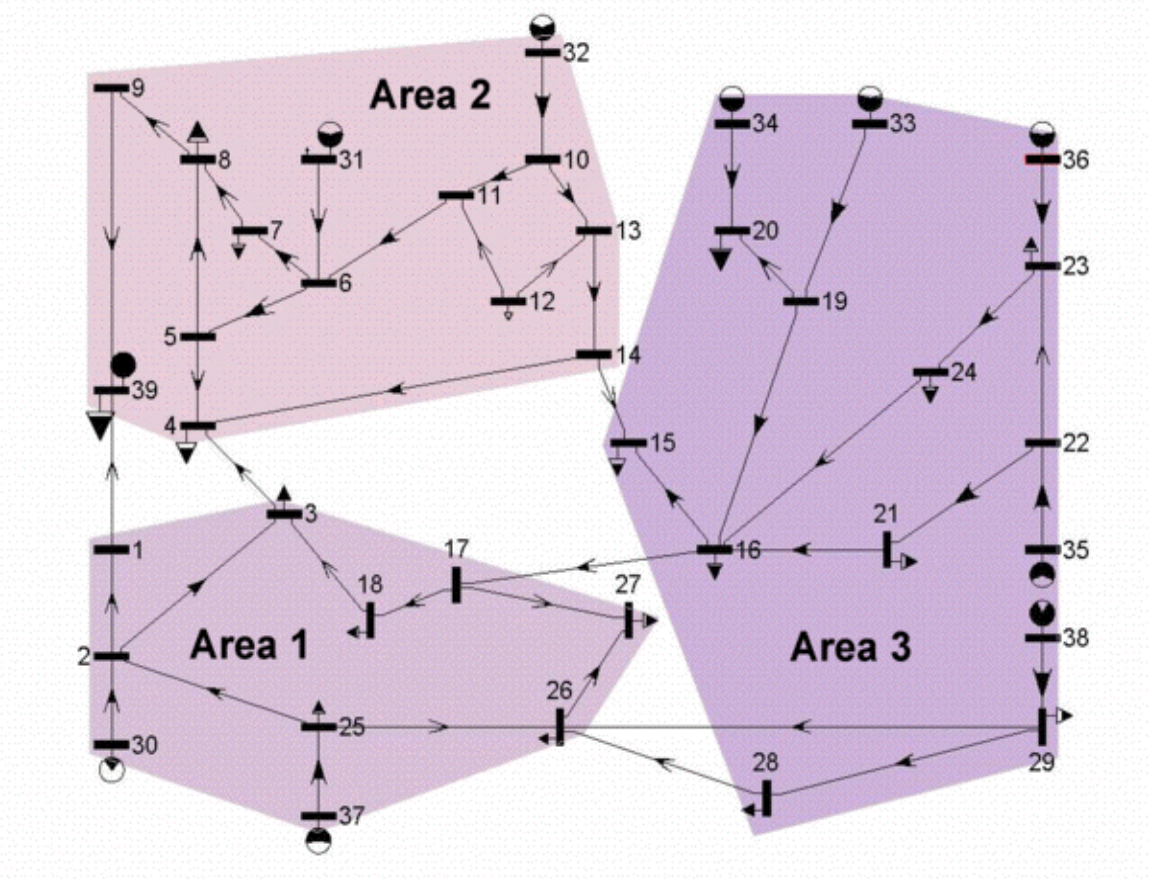

Figure 4.5: IEEE 39-Bus System

Table 4.1 ATC for transfer from bus 39 to 15

	ATC (MW)	Limiting Factor
Integrated System	395	Line 2 – 3
Area 1	393	Line 2 – 3
Area 2	1075	Line 14 – 15
Area 3	653	Line 15 – 16
Multi-Area System	393	Line 2 – 3

Table 4.2 and 4.3 presents ATC results for transfer from bus 35 to bus 17 and bus 32 to bus 15 respectively. The results obtained using integrated and multi-area solutions are comparable for both of these transfers.

Table 4.2 ATC for transfer from bus 35 to 17

	ATC (MW)	Limiting Factor
Integrated System	428	Line 16 – 21
Area 1	444	Line 16 – 17
Area 2	727	Line 13 – 14
Area 3	430	Line 16 – 21
Multi-Area System	430	Line 16 – 21

Table 4.3 ATC for transfer from bus 32 to 15

	ATC (MW)	Limiting Factor
Integrated System	401	Line 6 – 11
Area 1	650	Line 3 – 18
Area 2	400	Line 6 – 11
Area 3	820	Line 14 – 15
Multi-Area System	400	Line 6 – 11

The transfers studied so far are inter-area transfers. For example, transfer from bus 39 to bus 15 is taking place between area 2 and 3. Table 4.4 presents the results for transfer from bus 39 to bus 4, which is the transfer within area 2. The interesting fact here is that even though the transfer is taking place within area 2, the limiting factor for this transfer is in area 1, which is the thermal limit of line from bus 2 to bus 3. So actually the

ATC value calculated by area 1 is the smallest one, which is also a multi-area ATC solution and is comparable to the solution obtained by integrated system.

Table 4.4 ATC for transfer from bus 39 to 4

	ATC (MW)	Limiting Factor
Integrated System	355	Line 2 – 3
Area 1	356	Line 2 – 3
Area 2	1010	Line 4 – 5
Area 3	1050	Line 3 – 4
Multi-Area System	356	Line 2 – 3

4.5 Conclusion

This chapter presented a new method based on hierarchical structure to solve for ATC problem of a multi-area power system. The proposed method is such that minimal data exchange is required between areas making it very suitable for deregulated power system in which areas are reluctant to share their real-time data. In the proposed method, individual areas calculate ATC for a given power transaction considering limiting factors of their own area using REI equivalents of neighbor areas. Central entity coordinates the results obtained by individual areas to determine the ATC value of an interconnected power system. Simulation results obtained using IEEE 39-bus system validates that ATC values determined using integrated and proposed multi-area method are comparable.

CHAPTER FIVE

SUMMARY AND FUTURE RESEARCH

5.1 Summary

An attempt has been made in this dissertation to develop tools that can help operators in energy control centers to operate the grid reliably and securely. With the deregulation of power systems, the large scale power transactions between utilities have increased drastically. In this situation, operators in control room do need to monitor an interconnected grid on a wide area basis. The tools developed as a part of this research will also help operators to detect the large scale cascading failure of the system during the slow progression phase in which they can take corrective actions to avoid or reduce the impact of it. Among various tools used in control centers to study and operate the grid, state estimator and transfer capability calculator are the vital tools in evaluating the static security of the system. In order to monitor the large scale power transactions taking place over an interconnected system, a wide area state estimator and transfer capability calculator are required. But because of competitive wholesale market of power and for security reasons, utilities are reluctant to share data among each others to achieve such a wide area solution of state estimator and transfer capability. The algorithms developed in this dissertation to achieve wide area state estimator and transfer capability calculator are such that minimal data exchange is required between utilities and that they can be used in real-time.

In first part of dissertation, a new method based on two-level state estimation is presented to achieve wide area state estimation of an interconnected power grid. This

way, individual areas are allowed to run their own state estimator, without exchanging any real-time data with their neighbor areas. The central coordinator then coordinates state estimator results available from individual areas to bring them to a global reference. Generally, use of boundary injection measurements at coordinator level requires some real-time data exchange between individual areas and coordinator other than just state estimator results. The use of modified power injections at coordinator level is proposed and implemented to minimize the real-time data exchange. The use of measurements available from Phasor Measurement Units (PMUs) in state estimation is getting a lot of attention in the industry nowadays. This dissertation presented two methods to incorporate PMU measurements in state estimation. The use of PMU measurements is proposed and implemented to improve the accuracy of two-level state estimator in presence of short or low impedance transmission lines around the boundary network.

In second part of dissertation, a new iterative method is presented to calculate the transfer capability of power system that can be used in real-time. The limitations of existing transfer capability calculation methods are either they are very slow or not accurate making them unsuitable for real-time application. The new proposed method overcomes all these disadvantages and can be used in real-time. Lastly, a two-level transfer capability algorithm was presented to achieve available transfer capability of an interconnected power system. As explained for wide area state estimator, individual areas calculates transfer capability of their own system for a given power transaction. Central coordinator then coordinates results of each area to obtain multi-area ATC value. The

developed method uses REI-equivalents to keep the data exchange minimum between control areas.

5.2 Future Research

The research presented in this dissertation can be a good reference for some of the possible future work listed below.

- The hierarchical structure used in this dissertation can also be applied to study voltage and transient stability of an interconnected system.
- More work is needed to study optimal placement of PMUs on the system to improve the redundancy and accuracy of the state estimator.
- More work is needed to study application of PMU measurements for real-time operations such as transient and voltage stability studies, automatic generation control, automatic voltage control and special protection schemes.
- Transfer capability calculation in this dissertation only focused on static security limits. The algorithm presented can be expanded to include transient and voltage stability limits.

APPENDICES

Appendix A

Flowchart of Multi-Area State Estimation

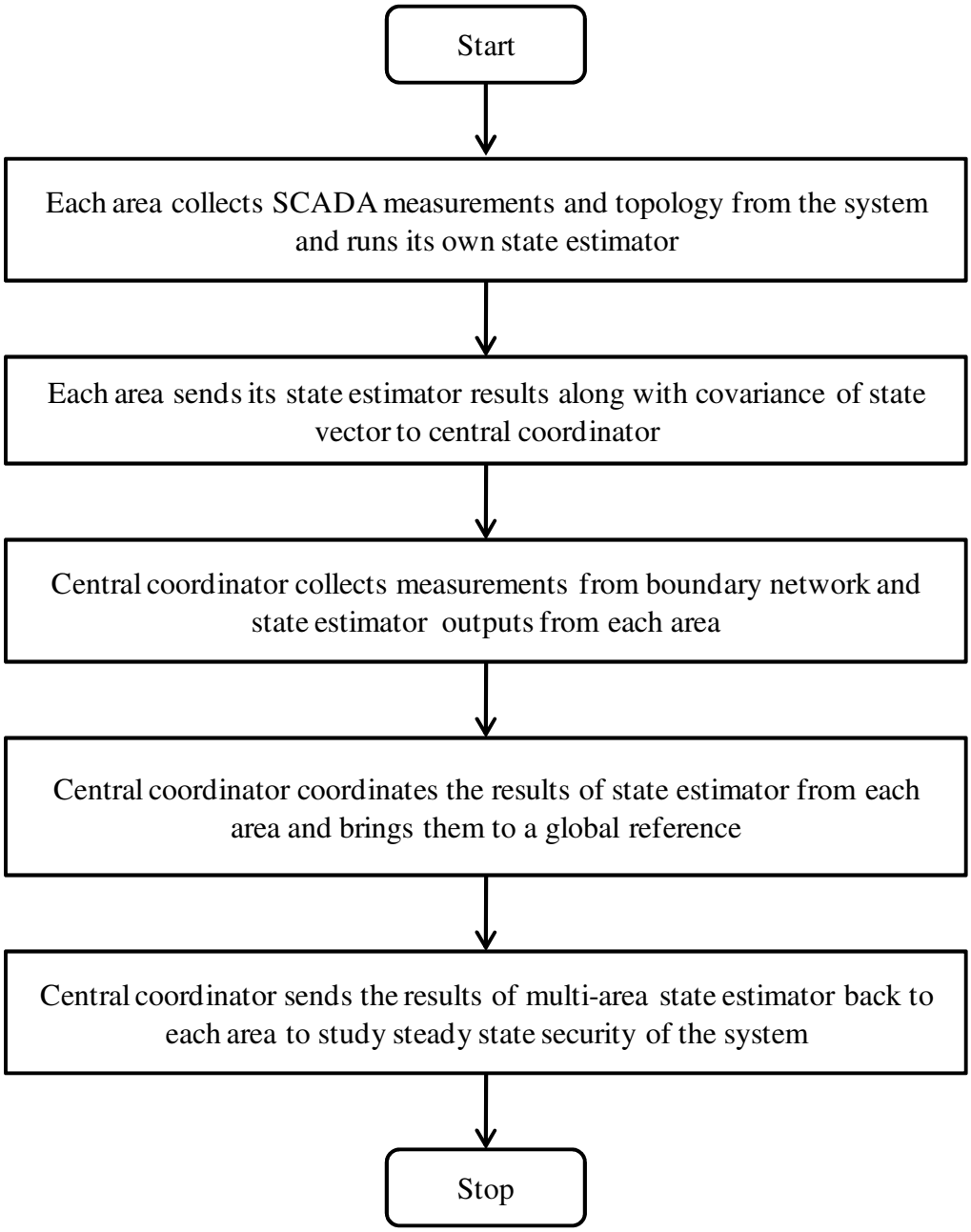

Figure A.1: Flowchart of Multi-Area State Estimation

Appendix B

Flowchart of Multi-Area ATC Calculation Method

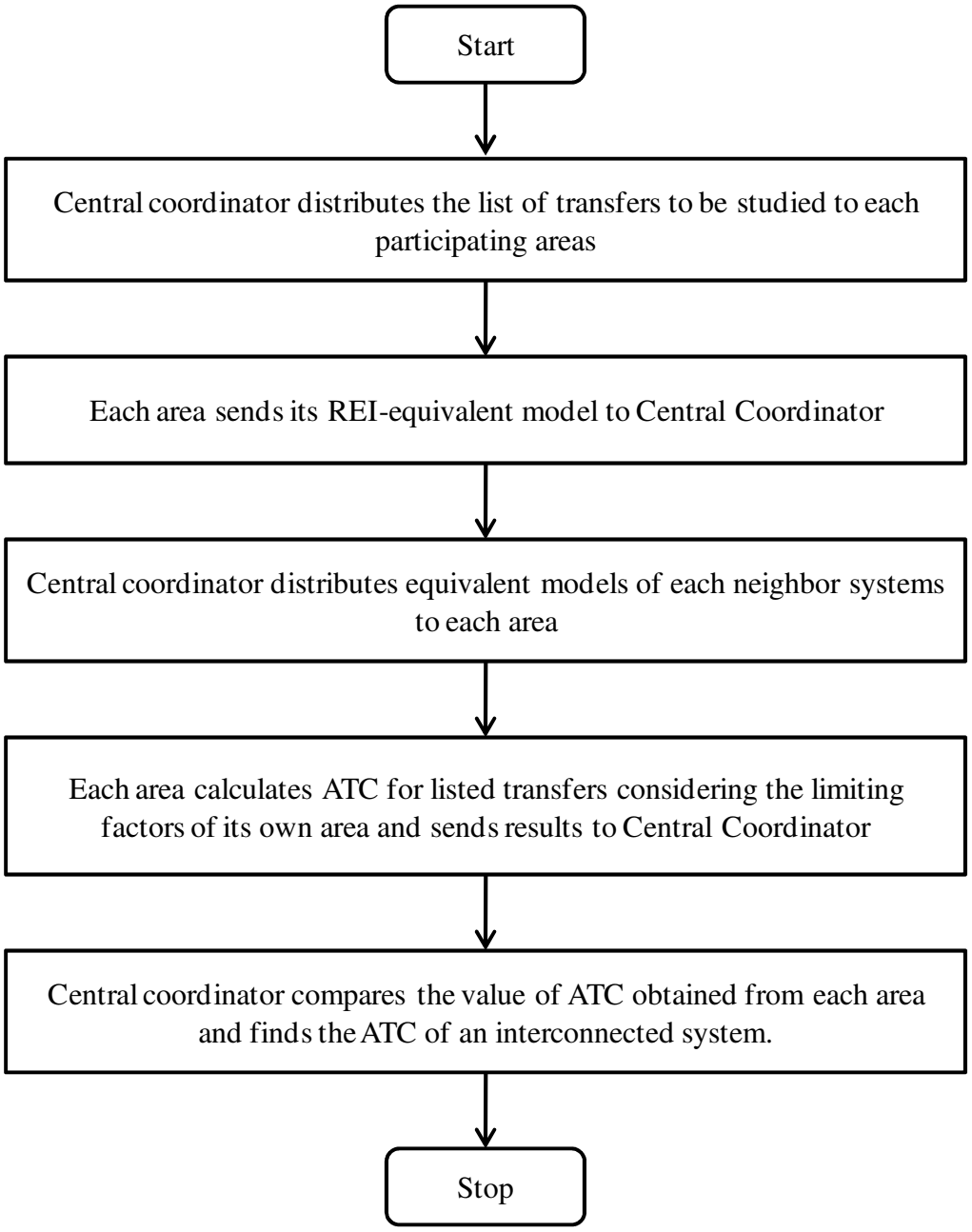

Figure B.1: Flowchart of Multi-Area ATC Calculation Method

Appendix C

MATLAB Program for State Estimation

RUNSE.m

```
clear all;

time = cputime;

% Reading the power flow result for the given system.
PF_result_30;

% forming the Ybus
Ybus26;
Ybus = sparse(Ybus);

nbus = length(Ybus(:,1)); % Total number of buses in system

nsv = 2*nbus-1; %Total number of State Variables in system

% Searching for the refenece bus
for n = 1:nbus
   if bus(n,2)==3
      rbus = n;
   end
end
rangle = bus(rbus,9)/57.32;  % Refernce bus angle

% Initializing the state vector Xs for flat start
for n = 1:nbus-1
   Xs(n,1) = 0;    % Initial Angles
end
for n = nbus:2*nbus-1
   Xs(n,1) = 1;    % Initial voltages
end

% Transferring from state vraibles to angles and voltages of the system.
for n=1:nbus
   if n<rbus
      ang(n,1)=Xs(n,1);
      else if n==rbus
         ang(n,1)=rangle;
         else
            ang(n,1) = Xs(n-1,1);
         end
   end
end

for n=1:nbus
   V(n,1) = Xs(nbus+n-1,1);
end
```

```
% forming the measurements

nmmt = 0; % Total number of measurements

% Extracting voltage from the power flow results

m = 0;
for n=1:nbus
   mmt(m+1,1)=0;
   mmt(m+1,2)=n;
   mmt(m+1,3)=0;
   mmt(m+1,4)=bus(n,8);
   m = m + 1;
end

nmmt=m;

% Extracting Bus Angles from Power Flow Results

m = 0;
for n=1:nbus
   if n ~= rbus
      mmt(m+1+nmmt,1)=5;
      mmt(m+1+nmmt,2)=n;
      mmt(m+1+nmmt,3)=0;
      mmt(m+1+nmmt,4)=bus(n,9);
      m = m +1;
   end
end

nmmt = nmmt + m;

%Extracting Power Injections from Power Flow Result

ngen = length(gen(:,1));  % Number of generators

for n=1:nbus
   PL(n,1) = bus(n,3);
   QL(n,1) = bus(n,4);
   PG(n,1) = 0;
   QG(n,1) = 0;
end

for n=1:ngen
   PG(gen(n,1),1) = gen(n,2);
   QG(gen(n,1),1) = gen(n,3);
end

for n=1:nbus
   QG(n,1)=QG(n,1)+bus(n,6);
end
```

```
m=0;

for n=1:nbus
      m=m+1;
      mmt(m+nmmt,1)=3;
      mmt(m+nmmt,3)=0;
      mmt(m+nmmt,4)=PG(n,1)-PL(n,1);
      mmt(m+nmmt,2)=n;
end

nmmt = nmmt + m;

m = 0;

for n=1:nbus
      m=m+1;
      mmt(m+nmmt,1)=4;
      mmt(m+nmmt,2)=n;
      mmt(m+nmmt,3)=0;
      mmt(m+nmmt,4)=QG(n,1)-QL(n,1);
end
nmmt = nmmt + m;

% Extracting Power Flows from the Power Flow Result

nbranch = length(branch(:,1));  % Number of branches

% Extracting Active Power Flow

for n=1:nbranch
   mmt(nmmt+n,1)=1;
   mmt(nmmt+n,2)=branch(n,1);
   mmt(nmmt+n,3)=branch(n,2);
   mmt(nmmt+n,4)=branch(n,12);
end

nmmt=nmmt+n;

for n=1:nbranch
   mmt(nmmt+n,1)=1;
   mmt(nmmt+n,2)=branch(n,2);
   mmt(nmmt+n,3)=branch(n,1);
   mmt(nmmt+n,4)=branch(n,14);
end

nmmt=nmmt+n;

% Extracting Reactive Power Flow

for n=1:nbranch
   mmt(nmmt+n,1)=2;
   mmt(nmmt+n,2)=branch(n,1);
```

```
   mmt(nmmt+n,3)=branch(n,2);
   mmt(nmmt+n,4)=branch(n,13);
end

nmmt=nmmt+n;

for n=1:nbranch
   mmt(nmmt+n,1)=2;
   mmt(nmmt+n,2)=branch(n,2);
   mmt(nmmt+n,3)=branch(n,1);
   mmt(nmmt+n,4)=branch(n,15);
end

nmmt=nmmt+n;


% Getting rid of Parallel Lines

for n = 1:nmmt
   if mmt(n,1)==1 | mmt(n,1)==2
      if mmt(n,2)==mmt(n-1,2) & mmt(n,3)==mmt(n-1,3)
         mmt(n-1,4) = mmt(n,4)+mmt(n-1,4);
         mmt(n,1) = 6;                    % This is the dummy Variable
      end
   end
end

temp = mmt;
clear mmt;
m=1;
for n = 1:nmmt
   if temp(n,1)~= 6
      mmt(m,:)=temp(n,:);
      m = m + 1;
   end
end
clear temp;
nmmt = length(mmt);


mvabase = 100;
d = mmt(:,1);
nl = mmt(:,2);
nr = mmt(:,3);
zm = mmt(:,4);


for i=1:nmmt
   if d(i)==0
      zm(i) = zm(i);
      else if d(i)==5;
         zm(i) = zm(i)/57.32;
         else
```

```
            zm(i) = zm(i)/mvabase;
        end
    end
end

% Initializing Weight matrix for Internal System

W = sparse([]);

W(nmmt,nmmt)=0;

for i=1:nmmt
        if d(i)==0   % for voltage measurements
            W(i,i) = 1/(0.01*0.01);
        end
        if d(i)==5  % for angle measurements
            W(i,i) = 1/(0.001*0.001);
        end
        if d(i)==1   % for active power flow measurements
            W(i,i) = 1/(0.015*0.015);
        end
        if d(i)==2   % for reactive power flow measurements
            W(i,i) = 1/(0.015*0.015);
        end
        if d(i)==3   % for active power injection measurements
            W(i,i) = 1/(0.03*0.03);
        end
        if d(i)==4   % for reactive power injection measurements
            W(i,i) = 1/(0.03*0.03);
        end
end


%************************************************************%
%% STARTING THE MAIN LOOP %%
%************************************************************%

for iter=1:15

    % Forming the Jacobian Matrix %

    % Intializing the Jacobian Matrix to zero

    H(nmmt,2*nbus-1)=0;
    T(nmmt,2*nbus)=0;

    for i=1:nmmt

        if d(i)==0
            for j =nbus:2*nbus-1
                if j==nbus+nl(i)-1
                    H(i,j) = 1;
                else
```

```
            H(i,j) = 0;
          end
        end
      end

      if d(i)==5
        for j=1:nbus-1
          if nl(i)<rbus
            if j == nl(i)
              H(i,j) = 1;
            else
              H(i,j) = 0;
            end
          end
          if nl(i)>rbus
            if j==nl(i)-1
              H(i,j) = 1;
            else
              H(i,j) = 0;
            end
          end
        end
      end


      if d(i)==1
        for j=1:nbus
          if j==nl(i)
            if A(nl(i),nr(i))~=0
              T(i,j) = A(nl(i),nr(i))*A(nr(i),nl(i))*(V(nl(i))*V(nr(i)))*[g(nl(i),nr(i))*sin(ang(nl(i))-
ang(nr(i))) - b(nl(i),nr(i))*cos(ang(nl(i))-ang(nr(i)))];
            else
              T(i,j) = (V(nl(i))*V(nr(i)))*[g(nl(i),nr(i))*sin(ang(nl(i))-ang(nr(i))) -
b(nl(i),nr(i))*cos(ang(nl(i))-ang(nr(i)))];
            end
          end
          if j==nr(i)
            if A(nl(i),nr(i))~=0
              T(i,j) = -(V(nl(i))*V(nr(i)))*A(nl(i),nr(i))*A(nr(i),nl(i))*[g(nl(i),nr(i))*sin(ang(nl(i))-
ang(nr(i))) - b(nl(i),nr(i))*cos(ang(nl(i))-ang(nr(i)))];
            else
              T(i,j) = -(V(nl(i))*V(nr(i)))*[g(nl(i),nr(i))*sin(ang(nl(i))-ang(nr(i))) -
b(nl(i),nr(i))*cos(ang(nl(i))-ang(nr(i)))];
            end
          end
        end

        for j=nbus+1:2*nbus
          if j==nbus+nl(i)
            if A(nl(i),nr(i))~=0
              T(i,j) = -V(nr(i))*A(nl(i),nr(i))*A(nr(i),nl(i))*[g(nl(i),nr(i))*cos(ang(nl(i))-
ang(nr(i)))+b(nl(i),nr(i))*sin(ang(nl(i))-
ang(nr(i)))]+2*A(nl(i),nr(i))*A(nl(i),nr(i))*(g(nl(i),nr(i))+gs(nl(i)))*V(nl(i));
```

```
                else
                    T(i,j) = -V(nr(i))*[g(nl(i),nr(i))*cos(ang(nl(i))-ang(nr(i)))+b(nl(i),nr(i))*sin(ang(nl(i))-
ang(nr(i)))]+2*(g(nl(i),nr(i))+gs(nl(i)))*V(nl(i));
                end
            end
            if j==nbus+nr(i)
                if A(nl(i),nr(i))~=0
                    T(i,j) = -V(nl(i))*A(nl(i),nr(i))*A(nr(i),nl(i))*[g(nl(i),nr(i))*cos(ang(nl(i))-
ang(nr(i)))+b(nl(i),nr(i))*sin(ang(nl(i))-ang(nr(i)))];
                else
                    T(i,j) = -V(nl(i))*[g(nl(i),nr(i))*cos(ang(nl(i))-ang(nr(i)))+b(nl(i),nr(i))*sin(ang(nl(i))-
ang(nr(i)))];
                end
            end
        end

        for j=1:2*nbus-1
            if j<rbus
                H(i,j) = T(i,j);
            else
                H(i,j) = T(i,j+1);
            end
        end
    end

    if d(i)==2
        for j=1:nbus
            if j==nl(i)
                if A(nl(i),nr(i))~=0
                    T(i,j) = -V(nl(i))*V(nr(i))*A(nl(i),nr(i))*A(nr(i),nl(i))*[g(nl(i),nr(i))*cos(ang(nl(i))-
ang(nr(i)))+b(nl(i),nr(i))*sin(ang(nl(i))-ang(nr(i)))];
                else
                    T(i,j) = -V(nl(i))*V(nr(i))*[g(nl(i),nr(i))*cos(ang(nl(i))-
ang(nr(i)))+b(nl(i),nr(i))*sin(ang(nl(i))-ang(nr(i)))];
                end
            end

            if j==nr(i)
                if A(nl(i),nr(i))~=0
                    T(i,j) = V(nl(i))*V(nr(i))*A(nl(i),nr(i))*A(nr(i),nl(i))*[g(nl(i),nr(i))*cos(ang(nl(i))-
ang(nr(i)))+b(nl(i),nr(i))*sin(ang(nl(i))-ang(nr(i)))];
                else
                    T(i,j) = V(nl(i))*V(nr(i))*[g(nl(i),nr(i))*cos(ang(nl(i))-
ang(nr(i)))+b(nl(i),nr(i))*sin(ang(nl(i))-ang(nr(i)))];
                end
            end
        end

        for j=nbus+1:2*nbus
            if j==nbus+nl(i)
                if A(nl(i),nr(i))~=0
                    T(i,j) = -V(nr(i))*[g(nl(i),nr(i))*sin(ang(nl(i))-ang(nr(i))) - b(nl(i),nr(i))*cos(ang(nl(i))-
ang(nr(i)))]-2*V(nl(i))*A(nl(i),nr(i))*A(nl(i),nr(i))*[b(nl(i),nr(i))+bs(nl(i))];
```

```
            else
               T(i,j) = -V(nr(i))*[g(nl(i),nr(i))*sin(ang(nl(i))-ang(nr(i))) - b(nl(i),nr(i))*cos(ang(nl(i))-
ang(nr(i)))]-2*V(nl(i))*[b(nl(i),nr(i))+bs(nl(i))];
            end
         end

         if j==nbus+nr(i)
            if A(nl(i),nr(i))~=0
               T(i,j) = -V(nl(i))*A(nl(i),nr(i))*A(nr(i),nl(i))*[g(nl(i),nr(i))*sin(ang(nl(i))-ang(nr(i))) -
b(nl(i),nr(i))*cos(ang(nl(i))-ang(nr(i)))];
            else
               T(i,j) = -V(nl(i))*[g(nl(i),nr(i))*sin(ang(nl(i))-ang(nr(i))) - b(nl(i),nr(i))*cos(ang(nl(i))-
ang(nr(i)))];
            end
         end
      end

      for j=1:2*nbus-1
         if j<rbus
            H(i,j) = T(i,j);
         else
            H(i,j) = T(i,j+1);
         end
      end
   end

   if d(i)==3
      for j=1:nbus
         if j==nl(i)
           T(i,j) = -V(j)*V(j)*B(j,j);
           for k = 1:nbus
              T(i,j) = T(i,j) + V(j)*V(k)*[-G(j,k)*sin(ang(j)-ang(k))+B(j,k)*cos(ang(j)-ang(k))];
           end
         else
            T(i,j) = V(nl(i))*V(j)*[G(nl(i),j)*sin(ang(nl(i))-ang(j))-B(nl(i),j)*cos(ang(nl(i))-ang(j))];
         end
      end
      for j=nbus+1:2*nbus
         if nl(i)+nbus==j
            T(i,j) = V(nl(i))*G(nl(i),nl(i));
            for k=1:nbus
               T(i,j) = T(i,j) + V(k)*[G(nl(i),k)*cos(ang(nl(i))-ang(k))+B(nl(i),k)*sin(ang(nl(i))-ang(k))];
            end
         else
            T(i,j) = V(nl(i))*[G(nl(i),j-nbus)*cos(ang(nl(i))-ang(j-nbus))+B(nl(i),j-nbus)*sin(ang(nl(i))-
ang(j-nbus))];
         end
      end
      for j=1:2*nbus-1
         if j<rbus
            H(i,j) = T(i,j);
         else
            H(i,j) = T(i,j+1);
```

```
            end
          end
       end

       if d(i)==4
          for j=1:nbus
             if j==nl(i)
               T(i,j) = -V(j)*V(j)*G(j,j);
               for k = 1:nbus
                  T(i,j) = T(i,j) + V(j)*V(k)*[G(j,k)*cos(ang(j)-ang(k))+B(j,k)*sin(ang(j)-ang(k))];
               end
             else
                T(i,j) = V(nl(i))*V(j)*[-G(nl(i),j)*cos(ang(nl(i))-ang(j))-B(nl(i),j)*sin(ang(nl(i))-ang(j))];
             end
          end
          for j=nbus+1:2*nbus
             if nl(i)+nbus==j
                T(i,j) = -V(nl(i))*B(nl(i),nl(i));
                for k=1:nbus
                   T(i,j) = T(i,j) + V(k)*[G(nl(i),k)*sin(ang(nl(i))-ang(k))-B(nl(i),k)*cos(ang(nl(i))-ang(k))];
                end
             else
                T(i,j) = V(nl(i))*[G(nl(i),j-nbus)*sin(ang(nl(i))-ang(j-nbus))-B(nl(i),j-nbus)*cos(ang(nl(i))-
ang(j-nbus))];
             end
          end
          for j=1:2*nbus-1
             if j<rbus
                H(i,j) = T(i,j);
             else
                H(i,j) = T(i,j+1);
             end
          end
       end
    end

% Final End of the Jacobian Loop

    HT = transpose(H);
    Gain = (HT*W*H);

% Finding error for internal Measurements

    zx = zeros(nmmt,1);
    error = zeros(nmmt,1);


    for i=1:nmmt
       if d(i)==0
         zx(i,1) = V(nl(i));
         error(i,1) = zm(i)-zx(i,1);
       end
```

```
      if d(i)==5
        zx(i,1) = ang(nl(i));
        error(i,1) = zm(i)-zx(i,1);
      end

      if d(i)==3
        for j=1:nbus
          zx(i,1) = zx(i,1) + V(nl(i))*V(j)*[G(nl(i),j)*cos(ang(nl(i))-ang(j))+B(nl(i),j)*sin(ang(nl(i))-
ang(j))];
        end
        error(i,1) = zm(i)-zx(i,1);
      end

      if d(i)==4
        for j=1:nbus
          zx(i,1) = zx(i,1) + V(nl(i))*V(j)*[G(nl(i),j)*sin(ang(nl(i))-ang(j))-B(nl(i),j)*cos(ang(nl(i))-
ang(j))];
        end
        error(i,1) = zm(i)-zx(i,1);
      end

     if d(i)==1
       if A(nl(i),nr(i))~=0
         zx(i,1) = [V(nl(i))*A(nl(i),nr(i))]^2*[g(nl(i),nr(i))+gs(nl(i),nr(i))]-
((V(nl(i))*V(nr(i)))*A(nl(i),nr(i))*A(nr(i),nl(i)))*[g(nl(i),nr(i))*cos(ang(nl(i))-ang(nr(i))) +
b(nl(i),nr(i))*sin(ang(nl(i))-ang(nr(i)))];
       else
         zx(i,1) = [V(nl(i))]^2*[g(nl(i),nr(i))+gs(nl(i),nr(i))]-
(V(nl(i))*V(nr(i)))*[g(nl(i),nr(i))*cos(ang(nl(i))-ang(nr(i))) + b(nl(i),nr(i))*sin(ang(nl(i))-ang(nr(i)))];
       end
       error(i,1) = zm(i) - zx(i,1);
     end

     if d(i)==2
       if A(nl(i),nr(i))~=0
         zx(i,1) = -[V(nl(i))*A(nl(i),nr(i))]^2*[b(nl(i),nr(i))+bs(nl(i),nr(i))]-
((V(nl(i))*V(nr(i)))*A(nl(i),nr(i))*A(nr(i),nl(i)))*[g(nl(i),nr(i))*sin(ang(nl(i))-ang(nr(i))) -
b(nl(i),nr(i))*cos(ang(nl(i))-ang(nr(i)))];
       else
         zx(i,1) = -[V(nl(i))]^2*[b(nl(i),nr(i))+bs(nl(i),nr(i))]-
(V(nl(i))*V(nr(i)))*[g(nl(i),nr(i))*sin(ang(nl(i))-ang(nr(i))) - b(nl(i),nr(i))*cos(ang(nl(i))-ang(nr(i)))];
       end
       error(i,1) = zm(i) - zx(i,1);
     end
   end

   BB = HT*W*error;
   delx = Gain\BB;

         %    U = chol(Gain);
         %    L = transpose(U);
         %    col = 1;
         %    row = length(BB(:,1));
```

```
        %
        %    % Solving using forward solution
        %    for j =1:col
        %       Y(1,j)=BB(1,j)/L(1,1);
        %       for i =2:row
        %          sum = 0;
        %          for k = 1:i-1
        %             sum = sum + L(i,k)*Y(k,j);
        %          end
        %          Y(i,j)=(BB(i,j)-sum)/L(i,i);
        %       end
        %    end
        %
        %    % Solving using backward solution
        %    for j =1:col
        %       x(row,j)=Y(row,j)/U(row,row);
        %       for i=row-1:-1:1
        %          sum =0;
        %          for k = i+1:row
        %             sum = sum + U(i,k)*x(k,j);
        %          end
        %          x(i,j)=(Y(i,j)-sum)/U(i,i);
        %       end
        %    end
        %
        %    delx = x;

   if max(abs(delx))<0.0001  % Criteria to stop the iteartions of the SE
     break;
   end

   Xs = Xs + delx;   % State after each iteration

   % Assigning the state variables to Voltages and Angles.

   for n=1:nbus
      if n<rbus
        ang(n,1)=Xs(n,1);
        else if n==rbus
              ang(n,1)=rangle;
        else
           ang(n,1) = Xs(n-1,1);
        end
       end
   end

   for n=1:nbus
      V(n,1) = Xs(nbus+n-1,1);
   end

   %clear U L Y  ;

end % END of Iterative loop
```

```
time = cputime - time;

for n=1:nbus
   perdelV(n,1) = ((V(n,1)-bus(n,8))/bus(n,8))*100;
end

for n=1:nbus
   if rbus==n;
      perdelANG(n,1)=0;
   else
   perdelANG(n,1) = ((ang(n,1)*57.32-bus(n,9))/bus(n,9))*100;
   end
end


mmt(:,5) = zx(:);

for n=1:nmmt
   if mmt(n,1)==0
      mmt(n,5) = mmt(n,5);
   else
      mmt(n,5) = mmt(n,5)*100;
   end
end

% Variance of the Estimate Vector

Rrhat = inv(Gain);
```

PF_RESULT_30.m

```
% Power flow result in a form of MATLAB file
%%-----  Power Flow Data  -----%%
%% system MVA base
baseMVA = 100;

%% bus data
%       bus_i   type    Pd      Qd      Gs      Bs      area    Vm      Va      baseKV  zone
        Vmax    Vmin
bus = [
        1       3       0       0       0       0       1       1       0       135     1
        1.05    0.95;
        2       2       21.7    12.7    0       0       1       1       -0.41549072     135
        1       1.1     0.95;
        3       1       2.4     1.2     0       0       1       0.98313829      -1.5220739
        135     1       1.05    0.95;
        4       1       7.6     1.6     0       0       1       0.980093        -1.7947277
        135     1       1.05    0.95;
        5       1       0       0       0       0.19    1       0.9824062       -1.8638227
        135     1       1.05    0.95;
        6       1       0       0       0       0       1       0.97318402      -2.2669567
        135     1       1.05    0.95;
```

```
        7       1       22.8    10.9    0       0       1       0.96735545      -2.6518368
        135     1       1.05    0.95;
        8       1       30      30      0       0       1       0.96062371      -2.7257694
        135     1       1.05    0.95;
        9       1       0       0       0       0       1       0.98050612      -2.9969331
        135     1       1.05    0.95;
        10      1       5.8     2       0       0       3       0.9844043       -3.3749359
        135     1       1.05    0.95;
        11      1       0       0       0       0       1       0.98050612      -2.9969331
        135     1       1.05    0.95;
        12      1       11.2    7.5     0       0       2       0.98546832      -1.5369116
        135     1       1.05    0.95;
        13      2       0       0       0       0       2       1       1.4761633       135
        1       1.1     0.95;
        14      1       6.2     1.6     0       0       2       0.97667683      -2.3080354
        135     1       1.05    0.95;
        15      1       8.2     2.5     0       0       2       0.98022903      -2.3118354
        135     1       1.05    0.95;
        16      1       3.5     1.8     0       0       2       0.97739566      -2.6444862
        135     1       1.05    0.95;
        17      1       9       5.8     0       0       2       0.97686541      -3.3923392
        135     1       1.05    0.95;
        18      1       3.2     0.9     0       0       2       0.96844033      -3.4783877
        135     1       1.05    0.95;
        19      1       9.5     3.4     0       0       2       0.96528704      -3.9582047
        135     1       1.05    0.95;
        20      1       2.2     0.7     0       0       2       0.96916635      -3.8710243
        135     1       1.05    0.95;
        21      1       17.5    11.2    0       0       3       0.9933833       -3.4883933
        135     1       1.05    0.95;
        22      2       0       0       0       0       3       1       -3.392729       135
        1       1.1     0.95;
        23      2       3.2     1.6     0       0       2       1       -1.5892279      135
        1       1.1     0.95;
        24      1       8.7     6.7     0       0.04    3       0.9885663       -2.6314615
        135     1       1.05    0.95;
        25      1       0       0       0       0       3       0.99021484      -1.6899889
        135     1       1.05    0.95;
        26      1       3.5     2.3     0       0       3       0.97219415      -2.139346
        135     1       1.05    0.95;
        27      2       0       0       0       0       3       1       -0.82843932     135
        1       1.1     0.95;
        28      1       0       0       0       0       1       0.9747149       -2.2659286
        135     1       1.05    0.95;
        29      1       2.4     0.9     0       0       3       0.9795967       -2.1284982
        135     1       1.05    0.95;
        30      1       10.6    1.9     0       0       3       0.96788288      -3.0415236
        135     1       1.05    0.95;
];

%% generator data
%       bus     Pg      Qg      Qmax    Qmin    Vg      mBase   status  Pmax    Pmin
gen = [
```

```
        1       25.9738 -0.998484       150     -20     1       100     1       80      0;
        2       60.97   31.999  60      -20     1       100     1       80      0;
        22      21.59   39.57   62.5    -15     1       100     1       50      0;
        27      26.91   10.5405 48.7    -15     1       100     1       55      0;
        23      19.2    7.95095 40      -10     1       100     1       30      0;
        13      37      11.3529 44.7    -15     1       100     1       40      0;
];

%% branch data
%       fbus    tbus    r       x       b       rateA   rateB   rateC   ratio   angle   status
        Pf      Qf      Pt      Qt
branch = [
        1       2       0.02    0.06    0.03    130     130     130     0       0       1
        10.8906 -5.0864 -10.8643 2.1652;
        1       3       0.05    0.19    0.02    130     130     130     0       0       1
        15.0832 4.0879  -14.9565-5.5730;
        2       4       0.06    0.17    0.02    65      65      65      0       0       1
        16.0673 5.2062  -15.8893-6.6624;
        3       4       0.01    0.04    0       130     130     130     0       0       1
        12.5565 4.3730  -12.5382-4.2998;
        2       5       0.05    0.2     0.02    130     130     130     0       0       1
        13.7919 4.5059  -13.6816-6.0299;
        2       6       0.06    0.18    0.02    65      65      65      0       0       1
        20.2751 7.4217  -19.9859-8.5011;
        4       6       0.01    0.04    0       90      90      90      0       0       1
        22.4991 11.3848 -22.4329-11.1200;
        5       7       0.05    0.12    0.01    70      70      70      0       0       1
        13.6816 6.2133  -13.5614-6.8753;
        6       7       0.03    0.08    0.01    130     130     130     0       0       1
        9.2700  3.1671  -9.2386 -4.0247;
        6       8       0.01    0.04    0       32      32      32      0       0       1
        24.8223 24.4281 -24.6942-23.9158;
        6       9       0       0.21    0       65      65      65      0       0       1
        5.7890  -3.3563 -5.7890  3.4556;
        6       10      0       0.56    0       32      32      32      0       0       1
        3.3080  -1.9179 -3.3080  2.0044;
        9       11      0       0.21    0       65      65      65      0       0       1
        0.0000  0.0000  0.0000  0.0000;
        9       10      0       0.11    0       65      65      65      0       0       1
        5.7890  -3.4556 -5.7890  3.5076;
        4       12      0       0.26    0       65      65      65      0       0       1
        -1.6716 -2.0225 1.6716  2.0411;
        12      13      0       0.14    0       65      65      65      0       0       1
        -37.0000-9.2558 37.0000 11.3529;
        12      14      0.12    0.26    0       32      32      32      0       0       1
        5.3878  0.8791  -5.3510 -0.7993;
        12      15      0.07    0.13    0       32      32      32      0       0       1
        9.4770  -1.0634 -9.4115 1.1851;
        12      16      0.09    0.2     0       32      32      32      0       0       1
        9.2636  -0.1010 -9.1841 0.2777;
        14      15      0.22    0.2     0       16      16      16      0       0       1
        -0.8490 -0.8007 0.8522  0.8036;
```

```
        16      17      0.08    0.19    0       16      16      16      0       0       1
        5.6841  -2.0777 -5.6534 2.1506;
        15      18      0.11    0.22    0       16      16      16      0       0       1
        9.1646  0.7597  -9.0678 -0.5661;
        18      19      0.06    0.13    0       16      16      16      0       0       1
        5.8678  -0.3339 -5.8457 0.3818;
        19      20      0.03    0.07    0       32      32      32      0       0       1
        -3.6543 -3.7818 3.6632  3.8026;
        10      20      0.09    0.21    0       32      32      32      0       0       1
        5.9156  4.6248  -5.8632 -4.5026;
        10      17      0.03    0.08    0       32      32      32      0       0       1
        3.3700  8.0130  -3.3466 -7.9506;
        10      21      0.03    0.07    0       32      32      32      0       0       1
        -2.2338 -11.6670 2.2775 11.7689;
        10      22      0.07    0.15    0       32      32      32      0       0       1
        -3.7548 -8.4827 3.8170  8.6159;
        21      22      0.01    0.02    0       32      32      32      0       0       1
        -19.7775-22.9689 19.8706 23.1551;
        15      23      0.1     0.2     0       16      16      16      0       0       1
        -8.8053 -5.2484 8.9147  5.4671;
        22      24      0.12    0.18    0       16      16      16      0       0       1
        -2.0976 7.7989  2.1758  -7.6815;
        23      24      0.13    0.27    0       16      16      16      0       0       1
        7.0853  0.8838  -7.0191 -0.7462;
        24      25      0.19    0.33    0       16      16      16      0       0       1
        -3.8568 1.7668  3.8918  -1.7060;
        25      26      0.25    0.38    0       16      16      16      0       0       1
        3.5464  2.3705  -3.5000 -2.3000;
        25      27      0.11    0.21    0       16      16      16      0       0       1
        -7.4382 -0.6645 7.5007  0.7840;
        28      27      0       0.4     0       65      65      65      0       0       1
        -6.1130 -6.0848 6.1130  6.3980;
        27      29      0.22    0.42    0       16      16      16      0       0       1
        6.1739  1.6840  -6.0838 -1.5120;
        27      30      0.32    0.6     0       16      16      16      0       0       1
        7.1224  1.6746  -6.9511 -1.3534;
        29      30      0.24    0.45    0       16      16      16      0       0       1
        3.6838  0.6120  -3.6489 -0.5466;
        8       28      0.06    0.2     0.02    32      32      32      0       0       1
        -5.3058 -6.0842 5.3414  4.3300;
        6       28      0.02    0.06    0.01    32      32      32      0       0       1
        -0.7704 -2.6998 0.7716  1.7547;
];
```

YBUS26.m

```
% This program is to form the Ybus

j=sqrt(-1); i = sqrt(-1);
nl = branch(:,1); nr = branch(:,2); R = branch(:,3);
X = branch(:,4); Bc = j*branch(:,5)/2; a = branch(:, 9);
nbr=length(branch(:,1)); nbus = max(max(nl), max(nr));
```

```
A = ones(nbus);
for n=1:nbr
   if branch(n,9)~=0
      if  A(nl(n),nr(n)) == 1
         A(nl(n),nr(n)) = 1/branch(n,9);
      else
         A(nl(n),nr(n)) =  (A(nl(n),nr(n))+(1/branch(n,9)))/2;
      end
   end
end

Z = R + j*X; y= ones(nbr,1)./Z;        %branch admittance
% Admittance of each branch
for n =1:nbus            % initialize Ybus to zero
      for m =1:nbus
         g(n,m)=0;b(n,m)=0;gs(n,m)=0;bs(n,m)=0;
      end
   end

for n=1:nbr
   if b(nl(n),nr(n))==0
      g(nl(n),nr(n)) = real(y(n));
      g(nr(n),nl(n)) = real(y(n));
      b(nl(n),nr(n)) = imag(y(n));
      b(nr(n),nl(n)) = imag(y(n));
   else
      g(nl(n),nr(n)) = g(nl(n),nr(n))+real(y(n));
      g(nr(n),nl(n)) = g(nr(n),nl(n))+real(y(n));
      b(nl(n),nr(n)) = b(nl(n),nr(n))+imag(y(n));
      b(nr(n),nl(n)) = b(nr(n),nl(n))+imag(y(n));
   end
end

for n=1:nbr
  if b(nl(n),nr(n))==0
      gs(nl(n),nr(n)) = real(Bc(n));
      gs(nr(n),nl(n)) = real(Bc(n));
      bs(nl(n),nr(n)) = imag(Bc(n));
      bs(nr(n),nl(n)) = imag(Bc(n));
   else
      gs(nl(n),nr(n)) = gs(nl(n),nr(n))+real(Bc(n));
      gs(nr(n),nl(n)) = gs(nr(n),nl(n))+real(Bc(n));
      bs(nl(n),nr(n)) = bs(nl(n),nr(n))+imag(Bc(n));
      bs(nr(n),nl(n)) = bs(nr(n),nl(n))+imag(Bc(n));
   end
end
%gs = real(Bc); bs = imag(Bc);
for n = 1:nbr
   if a(n) <= 0
      a(n) = 1;
   end
end
```

```
Ybus=zeros(nbus,nbus);     % initialize Ybus to zero
            % formation of the off diagonal elements
   for k=1:nbr
      Ybus(nl(k),nr(k))=Ybus(nl(k),nr(k))-y(k)/a(k);
      Ybus(nr(k),nl(k))=Ybus(nl(k),nr(k));
   end


 % formation of the diagonal elements
for  n=1:nbus
    for k=1:nbr
       if nl(k)==n
       Ybus(n,n) = Ybus(n,n)+y(k)/(a(k)^2) + Bc(k);
       elseif nr(k)==n
       Ybus(n,n) = Ybus(n,n)+y(k) +Bc(k);
       else, end
    end
end
Ybus = sparse(Ybus);
g = sparse(g);
b = sparse(b);
gs = sparse(gs);
bs = sparse(bs);

G = real(Ybus);
B = imag(Ybus);
clear Pgg
```

Appendix D

MATLAB Program for Available Transfer Capability Calculation

CalculateATC.m

```
clear all;

basemva = 100;

%Input the system data file

PF_result_39;

x=0;

Ybus26; % forming the Ybus

nbus = length(Ybus(:,1));

dp1 = 0.10; % Incremental Active Power
dp2 = 0.01;

% Searching for the refenece bus
for n = 1:nbus
   if bus(n,2)==1
      rbus = n;
   end
end

V = bus(:,8);
ang = bus(:,9);

ang = ang/57.2958;

dp = 0.10;

% Calculating Pre-Transfer Power Flow

nl = branch(:,1);
nr = branch(:,2);

for i=1:length(branch)

    if A(nl(i),nr(i))~=0
      pf(i,4) = [V(nl(i))*A(nl(i),nr(i))]^2*[g(nl(i),nr(i))+gs(nl(i),nr(i))]-
((V(nl(i))*V(nr(i)))*A(nl(i),nr(i))*A(nr(i),nl(i)))*[g(nl(i),nr(i))*cos(ang(nl(i))-ang(nr(i))) +
b(nl(i),nr(i))*sin(ang(nl(i))-ang(nr(i)))];
    else
      pf(i,4) = [V(nl(i))]^2*[g(nl(i),nr(i))+gs(nl(i),nr(i))]-(V(nl(i))*V(nr(i)))*[g(nl(i),nr(i))*cos(ang(nl(i))-
ang(nr(i))) + b(nl(i),nr(i))*sin(ang(nl(i))-ang(nr(i)))];
```

```
    end

end

pf(:,1) = branch(:,1);
pf(:,2) = branch(:,2);
pf(:,3) = branch(:,7);
pf(:,4) = pf(:,4)*100;

clear nl nr;

c =1;

for n=1:nbus
   if bus(n,2)==0 | bus(n,2)==2
      mmt(c,1)=3;
      mmt(c,2)=n;
      mmt(c,3)=0; mmt(c,4)=0;
      c=c+1;
   end
end
for n=1:nbus
   if bus(n,2)==0
      mmt(c,1)=4;
      mmt(c,2)=n;
      mmt(c,3)=0; mmt(c,4)=0;
      c=c+1;
   end
end


for mm = 1:30

d = mmt(:,1);
nl = mmt(:,2);
nr = mmt(:,3);
zm = mmt(:,4);

%Calculating Jacobin Matrix

for i = 1:length(mmt)
   if d(i)==3
         for j=1:nbus
            if j==nl(i)
               T(i,j) = -V(j)*V(j)*B(j,j);
               for k = 1:nbus
                  T(i,j) = T(i,j) + V(j)*V(k)*[-G(j,k)*sin(ang(j)-ang(k))+B(j,k)*cos(ang(j)-ang(k))];
               end
            else
               T(i,j) = V(nl(i))*V(j)*[G(nl(i),j)*sin(ang(nl(i))-ang(j))-B(nl(i),j)*cos(ang(nl(i))-ang(j))];
            end
         end
         for j=nbus+1:2*nbus
```

```
            if nl(i)+nbus==j
               T(i,j) = V(nl(i))*G(nl(i),nl(i));
               for k=1:nbus
                  T(i,j) = T(i,j) + V(k)*[G(nl(i),k)*cos(ang(nl(i))-ang(k))+B(nl(i),k)*sin(ang(nl(i))-ang(k))];
               end
            else
               T(i,j) = V(nl(i))*[G(nl(i),j-nbus)*cos(ang(nl(i))-ang(j-nbus))+B(nl(i),j-nbus)*sin(ang(nl(i))-
ang(j-nbus))];
            end
         end
      end

      if d(i)==4
         for j=1:nbus
            if j==nl(i)
              T(i,j) = -V(j)*V(j)*G(j,j);
              for k = 1:nbus
                 T(i,j) = T(i,j) + V(j)*V(k)*[G(j,k)*cos(ang(j)-ang(k))+B(j,k)*sin(ang(j)-ang(k))];
              end
            else
               T(i,j) = V(nl(i))*V(j)*[-G(nl(i),j)*cos(ang(nl(i))-ang(j))-B(nl(i),j)*sin(ang(nl(i))-ang(j))];
            end
         end
         for j=nbus+1:2*nbus
            if nl(i)+nbus==j
               T(i,j) = -V(nl(i))*B(nl(i),nl(i));
               for k=1:nbus
                  T(i,j) = T(i,j) + V(k)*[G(nl(i),k)*sin(ang(nl(i))-ang(k))-B(nl(i),k)*cos(ang(nl(i))-ang(k))];
               end
            else
               T(i,j) = V(nl(i))*[G(nl(i),j-nbus)*sin(ang(nl(i))-ang(j-nbus))-B(nl(i),j-nbus)*cos(ang(nl(i))-
ang(j-nbus))];
            end
         end
      end
end

for i = 1:length(mmt)
   if d(i)==3
      H(:,i) = T(:,nl(i));
   end
   if d(i)==4
      H(:,i) = T(:,nl(i)+nbus);
   end
end

% Finished calculating Jacobin

% Calculating change in Voltage Magnitudes and Angles

deltaT = zeros(length(mmt),1);

for n=1:length(mmt)
```

```
   if mmt(n,1)==3 & mmt(n,2) == 32
      deltaT(n,1) = dp1;
   end
   if mmt(n,1)==3 & mmt(n,2) == 39
      deltaT(n,1) = -dp1;
   end
end

dx = inv(H)*deltaT;

clear H T;

% Updating Voltage Magnitudes & Angles

for i = 1:length(mmt)
   if d(i)==3
      ang(nl(i),1) = ang(nl(i),1) + dx(i,1);
   end
   if d(i)==4
      V(nl(i),1) = V(nl(i),1) + dx(i,1);
   end
end


clear nl nr;

nl = branch(:,1);
nr = branch(:,2);

for i=1:length(branch)

    if A(nl(i),nr(i))~=0
      pf(i,5) = [V(nl(i))*A(nl(i),nr(i))]^2*[g(nl(i),nr(i))+gs(nl(i),nr(i))]-
((V(nl(i))*V(nr(i)))*A(nl(i),nr(i))*A(nr(i),nl(i)))*[g(nl(i),nr(i))*cos(ang(nl(i))-ang(nr(i))) +
b(nl(i),nr(i))*sin(ang(nl(i))-ang(nr(i)))];
    else
      pf(i,5) = [V(nl(i))]^2*[g(nl(i),nr(i))+gs(nl(i),nr(i))]-(V(nl(i))*V(nr(i)))*[g(nl(i),nr(i))*cos(ang(nl(i))-
ang(nr(i))) + b(nl(i),nr(i))*sin(ang(nl(i))-ang(nr(i)))];
    end

end

pf(:,5) = pf(:,5)*100;


for i=1:length(pf)
   if abs(pf(i,5))>pf(i,3)
      x=1;i
   end
end

for i=1:length(pf)
   if pf(i,3)-abs(pf(i,5)) < 5
```

```
        dp1 = 0.0025;
    end
end

dp = dp+dp1;

if x==1   % To break the loop
    break;
end

clear nl nr;

end
```

References

1. Promoting Wholesale Competition through Open Access Non-Discriminatory Transmission Services by Public Utilities; Recovery of Stranded Costs by Public Utilities and Transmission Utilities," Docket Nos. RM95-8-000 & RM-7-001, Order No. 888, April 24, 1996.
2. U.S. - Canada Power System Outage Task Force, "Interim Report: Causes of the August 14th Blackout in the United States and Canada", November 2003.
3. U.S. - Canada Power System Outage Task Force, "Final Report: Causes of the August 14th Blackout in the United States and Canada", April, 2004.
4. K. Geisler and Anjan Bose, "State estimation based external network solution for online security analysis," IEEE transaction on Power Appar. and Systems., Vol PAS-102, pp. 2447-2454, Aug 1983.
5. A. Monticelli and F. F. Wu, "A method that combines internal state estimation and external network modeling", IEEE transaction on Power Appar. and Systems., Vol PAS-104, pp. 91-103, Jan 1985.
6. G. N. Korres, "A partitioned state estimator for external network modeling", IEEE transaction on Power System. Vol 17. No. 3 Aug. 2002.
7. H. Kim and A. Abur, "Enhancement of external system modeling for state estimation", IEEE transaction on Power System. Vol 11. pp 1380-1386. Aug. 1996.
8. Kurzyn, M. S., "Real-time State Estimation for Large Scale Power Systems", IEEE Transaction on PAS, Vol. PAS-102, No. 7, pp. 2055-2065, July 1983.
9. Wallach, Y., Handschin, E., and Bongers, C., "An Efficient Parallel Processing Method for Power System State Estimation", IEEE Transaction on PAS, Vol. PAS-100, No. 11, Nov. 1981.
10. Th. Van Cutsem, J. L. Howard, M. Ribben-Pavella, "A Two-Level Static State Estimator for Electric Power Systems", IEEE Transactions on PAS, Vol. PAS-100, pp. 3722-3732, August 1981.

11. Liang Zhao, Ali Abur, “Multiarea State Estimation Using Synchronized Phasor Measurements”, IEEE Transactions on Power Systems, Vol 20, No. 2, pp. 611-617, May 2005.
12. “Available transfer capability definitions and determination,” Tech. Rep., North American Electric Reliability Council, Princeton, NJ, 1996.
13. I. Dobson, S. Greene, R. Rajaraman, C.L. Demarco, F.L. Alvarado, M. Glavic, J. Zhang, and R. Zimmerman, “Electrical power transfer capability: Concepts, applications, sensitivity, uncertainty,” Project Report, Power Systems Engineering Research Center, 2001.
14. G.L. Landgren, H.L. Terhune, and R.K. Angel, “Transmission interchange capability - analysis by computer,” *IEEE Transactions on Power Apparatus and Systems*, vol. 91, no. 6, pp. 2405–2414, May 1972.
15. G.C. Ejebe, J.G. Waight, M. Santos-Nieto, and W.F. Tinney, “Fast calculations of linear available transfer capability,” in *Proc. Power Industry Computer Applications Conf.*, 1999, pp. 255–260.
16. G.C. Ejebe, J. Tong, G.C. Waight, J.G. Frame, X. Wang, and W.F. Tinney, “Available transfer capability calculations,” *IEEE Transactions on Power Systems*, vol. 13, no. 4, pp. 1521–1527, November 1998.
17. V. Ajjarapu and C. Christy, “The continuation power flow: A tool for steady state voltage stability analysis,” *IEEE Transactions on Power Systems*, vol. 7, no. 1, pp. 416–423, February 1992.
18. H.W. Dommel and W.F. Tinney, “Optimal power flow solutions,” *IEEE Transactions on Power Apparatus and Systems*, vol. 87, no. 10, pp. 1866–1876, 1968.
19. J.A. Momoh, M.E. El-Hawary, and R. Adapa, “A review of selected optimal power flow literature to 1993 part ii: Newton, linear programming and interior point methods,” *IEEE Transactions on Power Systems*, vol. 14, no. 1, pp. 105–111, February 1999.

20. A. Monticelli, “A state estimation in electric power systems. A generalized approach”, Kluwer’s Power Electronics and power system serious, 1999, Chapter 10, pp.267-282.
21. Allen J. Wood, Bruce F. Wollenberg, “Power generation operation and control”, a Wiley interscience publication, 1996, Chapter 12 pp. 464-467.
22. Metrics for Determining the Impact of Phasor Measurements on Power System State Estimation, Eastern Interconnection Phasor Project, March 2006.
23. K.E. Martin, “IEEE Standard of Synchrophasors for Power Systems”, IEEE Transactions on Power Delivery, Vol. 13, No.1 January 1998.
24. Floyd Galvan, ““The Eastern Interconnect Phasor Project” IEEE PES conference and exposition Dallas, Texas May 2006.
25. M. J. Rice, G. T. Heydt, “Power System state estimation accuracy enhancement through the use of PMU measurements”, IEEE PES T&D Conference and Exposition, Dallas, Texas, May 2006
26. Van Cutsem and Ribbens Pavela, M., ‘Critical survey of Hierarchical methods for state estimation of electric power systems,’ IEEE Transaction on PAS, Vol. PAS-102, No.10, Oct 1983.
27. H. Kobayshi, S. Narita, and M.S.A.A. Hamman, “Model Coordination Method Applied to Power System Control and Estimation Problems”, Presented at the *Proc. IFAC/IFIP 4th Int. Conf. on Digital Computer Appl. to Process Control,* pp. 114-128, 1974.
28. Lin, S.Y., ‘A distributed state estimator for electric power systems’, IEEE Transactions for Power Systems, Vol. 7, No 2, May 1992.
29. Clements, K. A., Denison, O. J., Ringlee, R. J., ‘A multi-area approach to state estimation power systems,’ IEEE PES Summer meeting, San Francisco, Cal., Jul 1972.
30. Seidu, K., Mukai, H., ‘Parallel Multi-Area State Estimation,’ IEEE Transactions on PAS, Vol. PAS-104, No. 5, May 1985.

31. H. Mukai, 'Parallel Multi-Area State Estimation,' EPRI report EL-2218, Final Report for project 1764-1, 1982.
32. Sasaki, H., Aoki, K., Yokoyama, R., 'A Parallel Computation Algorithm for Static State Estimation by means of Matrix Inversion Lemma,' IEEE Transactions for Power Systems, Vol. 2, No. 3, Aug. 1987.
33. Fahim, M. A., 'Static state Estimator for Multi-Area Power System,' Proceeding of 17th Modeling and Simulation Conference, Pittsburg University, April 1986.
34. R.D. Christie, B.F. Wollenberg, and I. Wangersteen, "Transmission management in the deregulated environment," *Proc. IEEE*, vol. 88, no. 2, pp. 170–195, February 2000.
35. D. Manjuree, Elham Makram, "Investigation of distribution factors for bilateral contract assessment", Electric Power Systems Research 66 (2003) pp. 205 - 214
36. A. Kumar, S. C. Sirvastva, "AC Power Transfer Distribution Factors for Allocating Power Transactions in a Deregulated Market", IEEE Power Engineering Review, July 2002.
37. B. Gao, G.K. Morison, and P. Kundur, "Towards the development of a systematic approach for voltage stability assessment of large-scale power system," *IEEE Transactions on Power Systems*, vol. 11, no. 3, pp. 1314–1324, August 1996.
38. G.C. Ejebe, J. Tong, G.C. Waight, J.G. Frame, X. Wang, and W.F. Tinney, "Available transfer capability calculations," *IEEE Transactions on Power Systems*, vol. 13, no. 4, pp. 1521–1527, November 1998.
39. V. Ajjarapu and C. Christy, "The continuation power flow: A tool for steady state voltage stability analysis," *IEEE Transactions on Power Systems*, vol. 7, no. 1, pp. 416–423, February 1992.
40. C.A. Canizares and F.L. Alvarado, "Point of collapse and continuation methods for large acdc systems," *IEEE Transactions on Power Systems*, vol. 8, no. 1, pp. 1–8, February 1993.
41. H.S. Chiang, A.J. Flueck, K.S. Shah, and N. Balu, "Cpflow: A practical tool for tracing power system steady-state stationary behavior due to load and generation

variations," *IEEE Transactions on Power Systems*, vol. 10, no. 2, pp. 623–634, May 1995.

42. P. Bresesti, D. Lucarella, P. Marannino, R. Vailati, and F. Zanellini, "An OPF based procedure for fast TTC analyses," in *Proc. Power Eng. Soc. General Meeting*, 2002, vol. 3, pp. 1504–1509.
43. Y. Ou and C. Singh, "Assessment of available transfer capability and margins," *IEEE Transactions on Power Systems*, vol. 17, no. 2, pp. 463–468, May 2002.
44. L. Zhao and A. Abur, "Two-layer multi-area total transfer capability computation," in *Proc. IREP Symp.*, Cortina D'Ampezzo, Italy, August 23-27 2004.
45. T. Stoilov and K. Stoilova, *Noniterative Coordination in Multilevel Systems*, pp. 1–56, Norwell, MA: Kluwer Acdemic Publishers, 1999.
46. M. Shaaban, W. Li, H. Liu, Z. Yan, Y. Ni, and F. Wu, "ATC calculation with steady-state security constraints using benders decomposition," in *IEE Proc. On Generation, Transmission and Distributio*, September 2003, vol. 150, pp. 611–615.
47. L. Min, A. Abur, "Total Transfer Capability Computation for Multi-Area Power Systems", IEEE transactions on power systems, Vol. 21, No. 3m, August 2006.
48. S.M. Deckman, A. Pizzolante, A. Monticelli, B. Scott, and O. Alsac, "Studies on power system load flow equivalencing," *IEEE Transactions on Power Apparatus and Systems*, vol. 99, pp. 2301–2310, November 1980.
49. P. Dimo, *Nodal Analysis of Power System*, Turibrige Wells, Kent, U.K.: Abacus Press, 1975.
50. W.F. Tinney and W.L. Powell, "The REI approach to power network equivalents," in *Transl.: 1977 PICA Conf.*, Toronto, ON, Canada, May 1977, pp. 312–320.
51. S.C. Savulescu, "Equivalents for security analysis of power system," *IEEE Transactions on Power Apparatus and Systems*, vol. 100, pp. 2672–2682, May 1981.

52. M. L. Oatts, S. R. Erwin, J. L. Hart, “Application of the REI Equivalent for Operations Planning Analysis of Interchange Schedules“,*IEEE Transactions on Power Systems*, Vol. 5, No. 2, pp. 547-555, May 1990.